Measuring sperm whales via acoustics and photogrammetry

Abraham Growcott

A thesis submitted for the degree of

Master of Science

At the University of Otago, Dunedin,

New Zealand

June 2010

Abstract

The most common vocalisations heard from sperm whales are short, broadband clicks which often display a decaying, evenly spaced, multi-pulse structure. The time between these pulses (inter-pulse interval: IPI) represents the two-way time for a pulse to travel between the air sacs located at either end of the sperm whale's head. The IPI therefore, is measure of head length and via an allometric relationship, total length. In order to compare IPIs of known individuals to an independent measure of length, a new, boat-based fully digital stereo photogrammetric system was developed and its measurement accuracy assessed. A field test was conducted measuring objects of known length throughout a distance/angle network. Mean measurement error over the entire network was 0.82% and it was found that the largest contributor to measurement error was the repeated manual selection of conjugate points in stereo images. IPIs were measured using a newly developed software plugin[1] for Pamguard, an open-source software package for passive acoustic monitoring. The plug-in was based on the recently developed "bent horn" theory of sound production in sperm whales. Previous studies relating IPI to an independent measure of length have suffered from very small sample sizes. Therefore, this study measured 21 sperm whales off Kaikoura, New Zealand using the new photogrammetric and acoustic method. Both measurement methods produced results which were repeatable and more accurate than previously published studies (mean C.V = 1.57% and 0.63%, respectively). A new equation describing the relationship between IPI and total length was proposed. To further boost sample size, the IPI plugin was also used to measure IPIs from archived recordings of whales that had been measured with a previous photogrammetric system. This brought the total sample size of different whales with both IPI measurements and stereo photogrammetric measurements to 33. Finally the IPI plugin was used to estimate acoustically the growth rates of 29 seasonal resident sperm whales which had been repeatedly recorded between 1991 and 2009. Most whales showed an increase in IPI over time representing growth. For individuals that were recorded many times over several years von Bertalanffy growth curves fitted the data well (mean $r^2 = 0.83$; range = 0.13- 0.99). This is the first time growth has been estimated using an acoustic method and because it is non-lethal it has the potential to allow different types of questions related to growth to be investigated.

[1] Developed by Miller (2010).

Acknowledgements

Firstly, a big thanks to Steve Dawson for giving me the opportunity to study sperm whales. Your supervision style has been the perfect mixture of expert guidance and at the same time you have allowed me the freedom to learn things for myself. You have an endless supply of enthusiasm, smart arse comments and coffee, which I have all needed at some point to complete this thesis. The culture you have developed within the Marine Mammal lab is one of excellence and hopefully this boy from Otaki (not Levin) met these expectations.

Pascal Sirguey, well what a find you were in the Surveying department. After a field season trialling an inadequate measuring method, we needed something new and you were there to help out. The addition of you as a co-supervisor was a master stroke and the development of the stereo camera system both met and exceeded my expectations. Thanks for your 'english' lessons when I was writing up and for your open door policy, it has been a privilege working with you.

This project also owes so much to Brian Miller, you first introduced me to Kaikoura and showed me what field work was all about. Your programming skills are out of this world and you have always given me such great advice and took your time to explain many concepts to me which at first were well over my head. Thank you for giving so much, I wish you well.

Cheers Will Rayment for bearing the cold to help me in the field at Kaikoura last winter. You introduced me to the delicacy that is the Kaikoura custard bun and our numerous surf sessions were sick.

Thanks must also be given to Liz Slooten and Elanor Hutchison for helping me in the field and being great to people to hang with.

Back in the lab I was fortunate to be writing up at the exact same time as Riley Elliot. I know we made Steve's life a misery for a while by stock piling him with chapters to edit, but for me it made life a lot easier to have someone around to bounce ideas off and share a laugh with. Our banter sessions with the rest of the lab I already know I will miss. Cheers bro and good luck for your future adventures.

To all fellow class mates and staff of the marine science department, you guys rule, especially when you make cake.

To my family, you guys are my constant and I would have never been able to get to where I have without you all. Thank you for everything.

This project would not have been possible without the financial support of the New Zealand Whale and Dolphin Trust. Cheers.

Finally, Ashleigh thanks for hanging in Dunedin while I pursued my dream. Don’t worry bubs it’s not long know till we hit the sun and surf!!!

Table of Contents

List of figures

Chapter 1

Chapter 2

Chapter 3

Chapter 4

Appendix

List of tables

Chapter 2

Chapter 3

Chapter 4

Chapter 1: General introduction

1.1 Biology and distribution

The sperm whale (*Physeter macrocephalus*) is the largest species of toothed whales. They are the most sexually dimorphic of all cetaceans with the largest recorded male being 18.3 metres long, weighing 57.1 metric tonnes whereas the largest recorded female measured 12.5 metres long and weighed 24 metric tonnes (Rice, 1989). Sperm whales have a worldwide distribution across all latitudes (Rice, 1989), which tends to be correlated with oceanic features such as high productivity zones, steep bottom topography and oceanic fronts (Jaquet and Whitehead, 1996). Distribution is further differentiated by latitude. Nursery groups of females and their progeny are mainly restricted to tropical and sub-tropical waters between 40°N and 40°S (Rice, 1989). Males, however disperse from their natal group at around six years of age (Richard et al., 1996) and congregate with other males of similar age to form 'bachelor schools' (Best, 1979). As males increase in age they become more solitary and range to higher latitudes. In both hemispheres large males range to the edge of the pack ice and only return to the tropics to breed (Rice, 1989).

The sperm whale has the distinction of having the biggest nose in the animal kingdom and this organ can account for up to a third of the body length of a mature male (Nishiwaki et al., 1963). The anatomy of the sperm whale's nasal complex is homologous to that of smaller odontocetes and thus provides evidence that the organ is involved in sound production (Cranford, 1996). Cranford (1999) also proposed that the organ's immense size is due to evolutionary pressures primarily caused by the animal's feeding ecology and to account for the high degree of sexual dimorphism in the case of males, sexual selection.

1.2 Sperm whales found at Kaikoura

The sperm whales seen offshore of Kaikoura are almost always males. Since Otago University research began in 1990, sightings of females have only occurred twice (Richter et al., 2003). Across the 1963-4 whaling season, 191 sperm whales' were taken in the Cook Strait/Kaikoura region of which only five were females (Gaskin and Cawthorn, 1967). Sperm whale distribution off Kaikoura is correlated with water depth, with most sightings made over the Kaikoura Canyon and Conway Trench which typically has water depths in excess of 500 meters (Jaquet et al., 2000). Seasonal distribution varies, with summer sightings most commonly located over the Kaikoura canyon in water deeper than 1000 meters, whereas in

winter sightings are dispersed to include areas over the shallower Conway trough. It is hypothesised that this seasonal variation is due to changes in prey type or distribution (Jaquet et al., 2000).

Sperm whales are present year round off Kaikoura. Absences are only occasional and last for a few days at most (Jaquet et al., 2000). Two types of residency patterns exist within the population, "seasonal residents" remain within the study site for several days or weeks and are re-sighted in several field seasons, whereas "transients" remain in the study area for several hours or days (Childerhouse et al., 1995; Jaquet et al., 2000; Letteval et al., 2002). Letteval et al. (2002) has estimated that within the Kaikoura study area there are 13.8 whales present at any one time and that "residents" have a mean residence period of 42 days (Standard error = 10.3).

1.3 Anatomy of the sperm whales head

The sperm whale's head is dominated by the two acoustically linked compartments collectively called the spermaceti organ (Fig 1.1) (Cranford, 1999). The spermaceti sac is located in the top half of the head and extends from the distal air sac located approximately below the blowhole to the frontal air sac which lines the trough formed by the front of the skull (Harvey and Norris, 1972). This sac is filled with waxy fluid which was prized by whalers for its many commercial uses (Rice, 1989). The second compartment is situated below the spermaceti sac and is called the junk. It is comprised of approximately 20 lens shaped cavities which are also filled with spermaceti (Mohl, 2001). The entire spermaceti organ is surrounded by a high concentration of arterial vessels which are within the muscle-tendon layer. This suggests that the spermaceti organ can be actively manipulated (Melnikov, 1997). The blowhole is connected to the left nasal passage which passes down the left side of the spermaceti sac, through a hole in the skull, forming a direct path for respiration (Goold and Jones, 1995). The right nasal passage is connected to both air sacs at either end of the spermaceti sac and is flat and broad in appearance (Goold and Jones, 1995). Both nasal passages are connected to each other through airways located at the frontal sac and near the blowhole allowing air to be recycled when producing clicks whilst diving (Goold and Jones, 1995). The sound producing organ, called the museau de singe (monkey muzzle), is located behind the distal sac in the spermaceti sac. It is comprised of a valve that looks like a set of lips that are almost as wide as the distal air sac (Norris and Harvey, 1972).

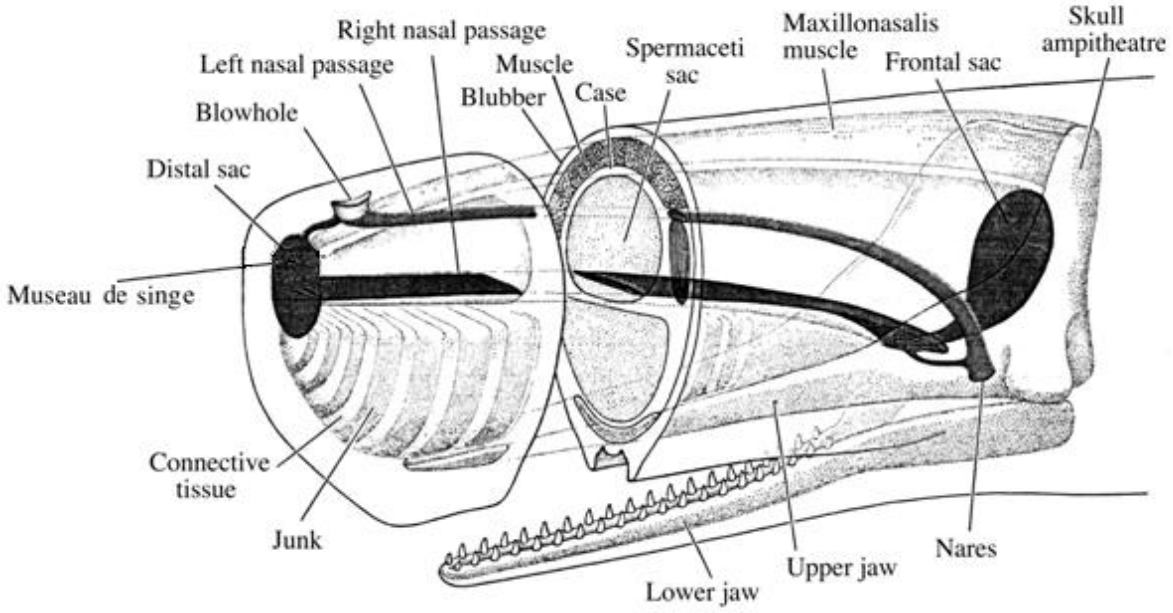

Figure 1.1 Diagram of the anatomy of the spermaceti organ (modified from Clarke, 1979)

1.4 Sound production

Norris and Harvey first proposed a theory to explain the mechanism of sound production in sperm whales in 1972. They hypothesised that clicks are produced by pneumatic action within the museau de singe. The majority of the energy within the click propagates forward and into the water column to form the P1 pulse. The remaining propagates backwards through the spermaceti sac and is reflected off the frontal air sac, due to the acoustic impedance between air and the spermaceti oil (Goold and Jones, 1995). This reflected energy is then transmitted into the water column to form the P2 pulse. The distal air sac intercepts a portion of the P2 pulse and reflects it so that it again travels through the spermaceti organ. This pattern continues until the sound energy diminishes (Rhinelander and Dawson, 2004).

Implicit in this hypothesis is the idea that the time delay between successive pulses (called the interpulse interval, IPI) within a single click is a measure of the distance between the two air sacs located at either end of the whales head (eq.1.1). Because head length is correlated to total length (Nishiwaki et al., 1963), they proposed that the IPI could be used for remote size estimation:

$$\text{Length of spermaceti organ (m)} = \frac{0.5(\text{IPI})}{\text{Speed of sound in spermaceti organ (m /sec)}}. \qquad (1.1)$$

This initial model of sound production has been modified by Mohl (2001) and Mohl et al. (1981; 2003) and is called the bent horn theory which has been supported further by Zimmer et al. (2005[a,b]). This model proposed that there is a weak pulse, P0 (Fig 1.2), which is produced by the museau de singe and exits directly into the water column possibly omni-directionally (Zimmer et al., 2005[a]) and contains a very small proportion of the total energy of the click. The majority of the energy (99.6%; Mohl et al., 2003) is contained in the P1 pulse. This pulse propagates posteriorly through the spermaceti sac and is reflected off the frontal sac, passing back through the junk to be emitted in the water column (Madsen et al., 2003; Møhl et al., 2003). Subsequent pulses of decaying amplitude are caused by the distal air sac intercepting a portion of the energy propagating through the junk before it enters the water column. This modification to the original Norris and Harvey theory does not alter the prediction that the IPI is the two way travel time between the air sacs when clicks are recorded on the body axis of the whale, i.e. in front or behind and thus can be an estimator of sperm whale length. This model also explains the irregular pulse structure of clicks recorded off-axis. This off-axis click structure will be further explained in the section titled, New Method for IPI Estimation.

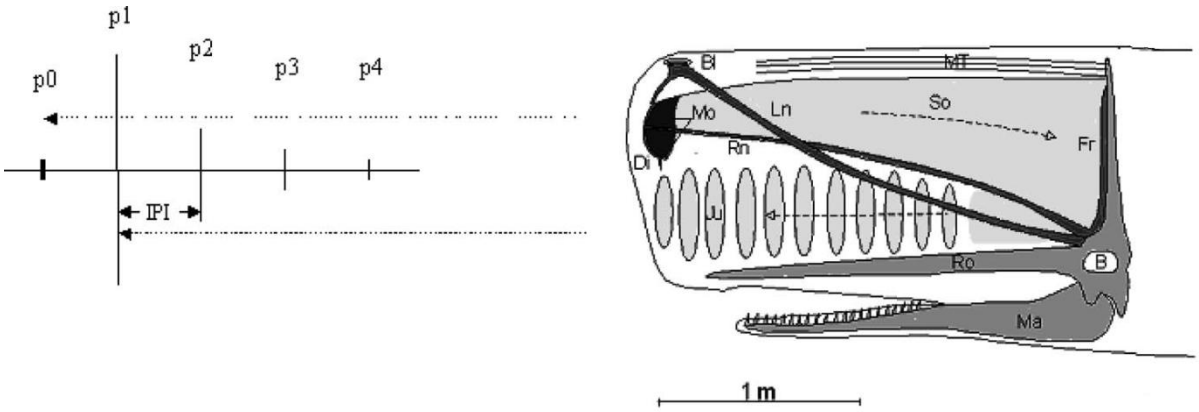

Figure 1.2 Schematic of a sperm whale head, showing the sound pathway of a click as predicted by the bent horn theory (from Zimmer et al., 2005[b]). B, brain; Bl, blow hole; Di,distal air sac; Fr, frontal air sac; Ju, junk; Ln, left naris; Ma, mandible; Mo,monkey lips/museau de singe; MT muscle/tendon layer; Rn, right naris; Ro, rostrum; So, spermaceti organ. The pulse structure of a forward facing on-axis click is displayed; showing the relative level of each pulse and constant spacing of the IPI.

1.5 Vocal repertoire and associated characteristics

Sperm whales are extremely vocal animals with males at Kaikoura emitting clicks 84.5% of the time when submerged (Jaquet et al., 2001). These clicks are characterised as being broadband and short in duration (Backus and Schevill, 1966; Fig 1.3). They are divided into four types (Whitehead, 2003) depending on the time delay between subsequent clicks which is called the inter-click interval (ICI). The most common click pattern is called 'Usual' clicks which have an ICI of between 0.5-2 seconds (Goold and Jones, 1995; Jaquet et al., 2001). Rapid click buzzes labelled creaks (Gordon, 1987) have a much faster repetition rate with an ICI ranging from 0.005-0.1 seconds (Whitehead, 2003). Codas and slow clicks have an ICI of 0.1-0.5 and 5-8 seconds respectively (Whitehead, 2003).

Usual clicks have been widely assumed to be used for echolocation. Several earlier studies found that usual clicks were of a moderate intensity of between 162-180 dB *re*: 1 μPa (Dunn, 1969; Levenson, 1974; Watkins, 1980). Watkins (1980) also argued that clicks were not highly directional and the click spectrum contained relatively low frequencies (2-8 kHz) which suggests that clicks were not used for echolocation.

Whitney (1968) and recent studies using large-aperture hydrophone arrays have found much higher source levels of between 223-235 kHz (Madsen et al., 2002; Mohl et. al., 2000; 2003), a high degree of directionality (Mohl et al., 2000; 2003; Zimmer et. al., 2005[a]) and click spectrum peaks in the 10-15 kHz range (Mohl et. al., 2003; Thode et al., 2002). These acoustic properties favour a bio-sonar function. The cause for this discrepancy is that clicks are seldom recorded on the longitudinal axis of the whale i.e. either directly in front or behind. Further, single hydrophone recordings cannot be used to deduce the orientation of the whale (Mohl et. al., 2000; 2003). When the orientation is known, however, on-axis clicks can be distinguished and their properties analysed (Mohl et al., 2000; 2003; Zimmer et al., 2005[a]). Additionally, the dynamics of click production is consistent with their use in echolocation and is similar to that seen in other echolocating animals (e.g. dolphins, bats, Jaquet et al., 2001).

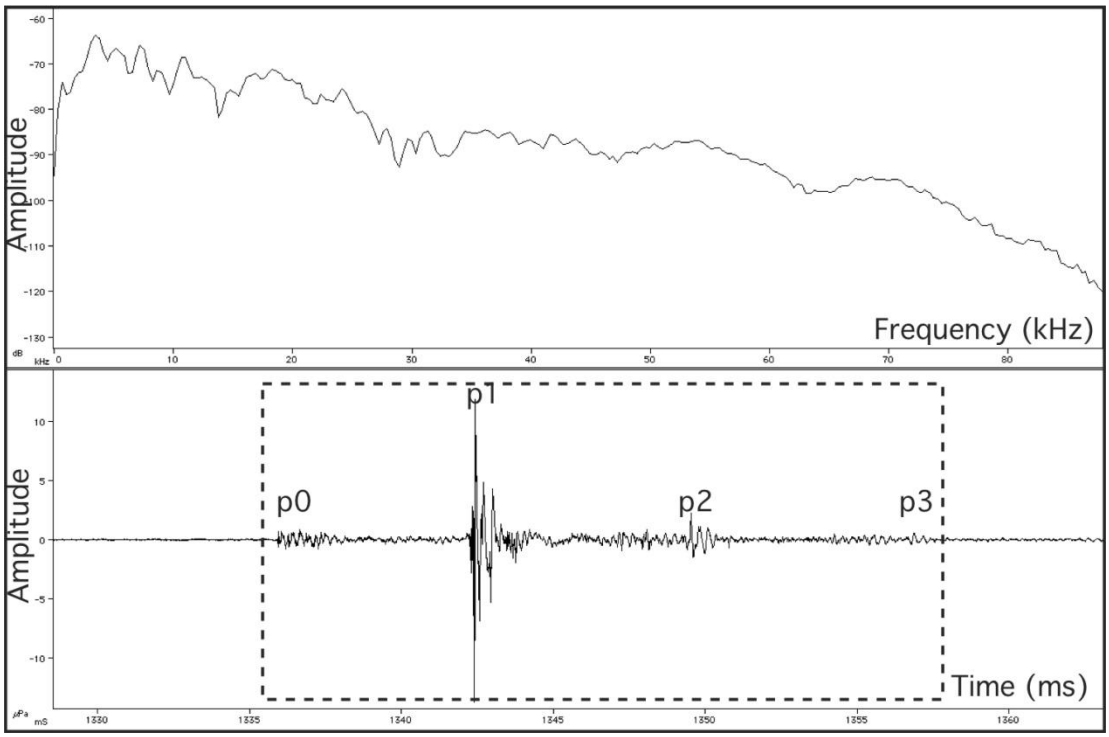

Figure 1.3 Structure and spectrum of a click recorded on-axis from a sperm whale oriented directly at the hydrophone at a range of c. 40m. The recording was made with a wideband recording system (150Hz-150kHz +/-4dB). The p0, p1, p2 and p3 pulses are shown. The dashed box indicates the time over which the spectrum is calculated (512pt FFT, analysing filter bandwidth 1398Hz).

1.6 Previous acoustic estimates of sperm whale length

Norris and Harvey (1972) were the first to compare the IPI measurement to a visual length estimate of the same whale. They concluded that an IPI of 2 ms related to a spermaceti sac length of 2.6 m using their equation (eq. 1.1). To estimate total body length they used the measurements of body proportions from Nishiwaki et al. (1963), which were derived from whaling records, to get a total body length of nine metres, which was very similar to their visually estimated length. The key weakness in this approach was that whale length was estimated visually, not measured, and hence of unknown accuracy.

Amundin (1978) used Norris and Harvey's IPI method to estimate an acoustic length of 22 m for a sperm whale that was visually estimated to be 21 m long. As above, whale length was not measured. Also, the acoustic length estimate is larger than any other measurement that has been made since, and larger than any total length measurement made in whaling (Rice, 1989).

Mohl et al. (1981) used data from the three above sources to develop the equation;

$$\text{Total length (TL)} = 0.86 + 4.53\ \text{IPI} - 0.142(\text{IPI}\cdot 1.3)^2 . \quad (1.2)$$

This equation was used by Alder-Fenchel (1980) to estimate the IPI within 41 click series recorded from various locations in the North Atlantic. A mean IPI was calculated from each series and resulted in total lengths ranging from 7-22 meters. The main assumption was that each series of clicks was assumed to be from a different whale and as before none of the recorded whales were independently measured.

Gordon (1991) measured the IPI of 11 individual from the Azores and around Sri Lanka. Unlike his predecessors, he had independent measures of the same whale, which were derived from a simple photogrammetric technique. The acoustic total lengths found using Mohl et al.'s (1981) equation were 1-6 meters longer than the photogrammetric estimates. Gordon (1991) suggested two main problems that could cause the overestimation. The first of these is that initial estimates of the speed of sound in spermaceti (Norris and Harvey, 1972) appear to have been too large by a factor of about two (Morris,1973,1975; Flewellen & Morris 1978; see also Goold, 1996), most likely due to an arithmetical error (Gordon, 1991). The second problem was that Mohl et al.'s (1981) equation used severed head length as a proxy for spermaceti sac length. This will introduce bias as the former is necessarily longer than the latter.

In light of these errors Gordon (1991) proposed two new equations. The first uses the relationship between spermaceti sac length and total length from five whales in Clarke (1978) and an average speed of sound in the spermaceti of 1372 msec^{-1} from Flewellen and Morris (1978). The equation is:

$$\text{TL} = 9.75 - 0.521\cdot\text{SL} + 0.068\cdot\text{SL}^2 + 0.057\cdot\text{SL}^3. \quad (1.3)$$

Where SL is obtained from equation 1.1.

The acoustic estimates fit a lot better when this equation is used. The second equation was proposed because the sample size of five whales in Clarke (1978) was so small. This equation was the first to empirically state the relationship between the IPI and independent length measurements gained from 11 individuals and is as follows:

$$\text{TL} = 4.833 + 1.453\cdot\text{IPI} - 0.001\cdot\text{IPI}^2. \quad (1.4)$$

Several studies have used Gordon's equation to estimate body lengths from IPIs (e.g. Pavan et al., 2000; Rendell and Whitehead, 2002; Drouot et al., 2004; Marcoux et al., 2006) but all these studies suffer from the lack of an independent estimate of whale size. Thus they are relying on Gordon's (1991) sample, which was relatively small (11) and contained only one individual over 12m.

Rhinelander and Dawson (2004) recorded sperm whale vocalisations offshore of Kaikoura, New Zealand and made independent measurements with a boat-based stereo photogrammetric system (Dawson et al., 1995). This study took repeated measurements of the same individuals over time and found that IPIs varied between individuals with most individuals showing significant increases in IPIs over several years, consistent with growth. This was the first study to validate that IPIs increase over time. Also, it was able to include data gained from larger whales than were previously measured (up to 15.3m; as measured via stereo photogrammetry). A new regression equation was also proposed based on the measurements of 12 individuals. This equation was:

$$TL = 22.268 - 3.629 \cdot IPI + 0.346 \cdot IPI^2. \quad (1.5)$$

1.7 Past IPI estimation methodologies

Gordon (1991) and all previous studies used oscilloscopes to display the waveform of recorded clicks. The time between pulses was measured manually and the IPI calculated. The problem with this method is that click waveforms which clearly display the signature multi-pulsed structure are uncommon (Goold, 1996). This makes choosing which clicks to measure subjective, resulting in measurements that could be imprecise.

Goold (1996) tested cross correlation and cepstrum analysis as new ways to measure IPIs in a less subjective manner. In cross-correlation a time shifted replica of a click is slid by the original and peaks in the correlation function will be highest when the P1 pulse of the second waveform aligns with the P2 pulse of the first. Measuring the time at which these align is equal to the IPI. Cepstrum, analysis however, is based in the frequency domain. Signals which contain pulses exhibit ripples in the spectrum and the period of these ripples equals the IPI (Rhinelander, 2001). Both these methods were unable to make accurate measurements within a single click due to the varying nature of signal quality. If however several hundred clicks were measured and then averaged, both methods would allow realistic estimates to be

obtained (Goold, 1996). Most studies published since 1996 have used either method, or both, to estimate the IPI of an individual whale.

As mentioned previously it is rare for a click to display a clear multi-pulsed structure. For example Alder-Fenchel (1980) found that only 11% of recorded clicks were suitable for analysis. Gordon (1991) and Goold (1996) suggested that click structure was influenced by two factors, physical distortion by the whale's head, and by the relative orientation of the whale with regard to the hydrophone. The latter is called off-axis distortion.

The methods were applied manually to each click and hence are time consuming. Also clicks that do not have a clear multi-pulsed structure are not used in analysis, rendering a large proportion of data collected useless. Clearly a new method of IPI estimation is needed.

1.8 A new method for IPI estimation

Zimmer et al. (2005[b]) created a geometric model of sound production based on the bent horn theory, which can account for the varying characteristics of off-axis clicks. They used a towed hydrophone array and attached a DTAG to the diving whale. This method enabled the whale's clicks to be examined from a fixed position (DTAG on dorsal fin) and in the far-field (towed hydrophone). Comparison between these two recording media showed that the P1 pulse does exit through the junk and that the P0 pulse exits close to the museau de singe. They also describe a new pulse (P1/2) which is evident in off-axis recordings. This pulse is created by the reflection of the P1 pulse off the frontal sac (Fig 1.4). The P1/2 position within a click is not static and can merge with either the P0 pulse when recorded behind the whale or the P1 pulse when recording in front of the whale. It can also be between the two pulses to varying degrees depending on the off-axis angle with respect to the hydrophone. This study highlighted that IPIs are aspect dependent and therefore a single click recorded from an unknown aspect cannot be used to reliably estimate an individual's length.

Following on from this finding, Teloni et al. (2007) developed a semi-automated method to estimate IPIs from a single element hydrophone recording using cepstrum analysis. IPI estimation is possible only if the cepstrums of a large number of clicks are computed and averaged. This is because clicks from a long click chain will be recorded from varying aspects, ranges and depths (Teloni et al., 2007) with respect to the hydrophone. The aspect dependent IPIs will slowly change throughout the recording, however the whale's 'true IPI' will always be present in every click. By averaging all the clicks' cepstra, the aspect

dependant IPIs will tend to cancel out, and the 'true IPI' will be left as an estimator of the whale's spermaceti sac length (Teloni et al., 2007).

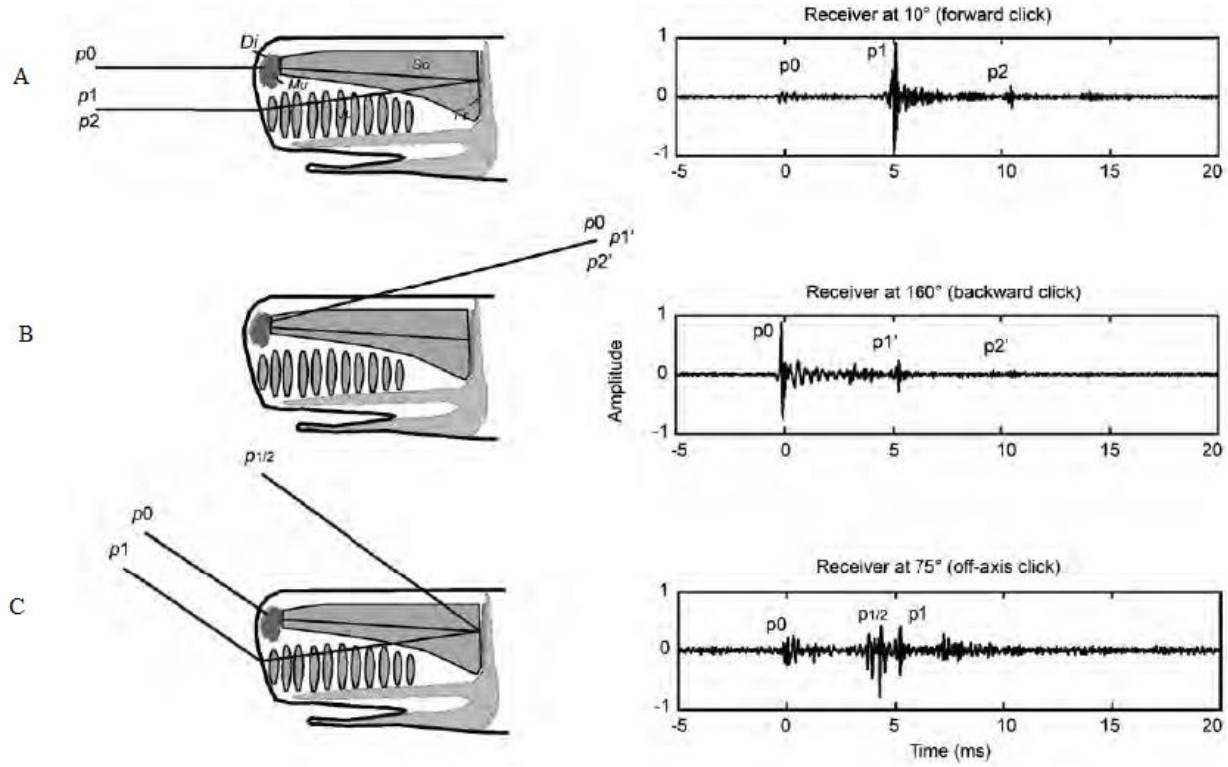

Figure 1.4 Diagram of a sperm whale's head (left) and associated pulse structure of usual clicks when recorded in the far-field from different bearings. A) On axis click when recorded in front of the whale; B) On axis click recorded from behind the whale; C) Off-axis click recorded at a 75^0 angle. The P1 and P2 pulse are shown as the same line for simplicity (from Teloni et al., 2007).

1.9 Non-acoustic length estimate techniques

The studies by Gordon (1991) and Rhinelander and Dawson (2004) have been the only ones to include a robust, non-acoustic measure of whale size. However the empirical relationships, that they have developed relating IPI to independent measures of whale length are based on relatively small sample sizes. If IPI measurements are to be used to document size structure, and growth, clearly the relationship needs to be based on more data. The problem here is that cetaceans are difficult to measure in their natural habitat and visual estimations usually overestimate length (Ohsumi, 1966). Most of data regarding the length of cetaceans is provided by whaling records. The International Whaling Commission's minimum catch lengths required routine measurement of catches, and these data extend to include other body

proportions (e.g. Fujino, 1956). In combination with age data gained from counting the annual laminations (GLGs) present in teeth, age-length growth curves were created (Nishiwaki 1963). These growth curves combined with the whaling measurements allow an individual's age and total length to be estimated from non-invasive measurements of particular body dimensions (e.g. Rhinelander and Dawson, 2004).

Various photographic methods have been employed to estimate the length of whales. There are three general approaches to photogrammetry, which use either (a) a single image with something of known size in the image to provide scale (b) a single image plus an accurate range measurement, or (c) stereo images.

Gordon (1991) took photos at a known height above the sea surface of sperm whales which were perpendicular to the boat. The angle between the horizon and the whale was measured on the developed film and the range was calculated from the curvature of the earth. The coefficient of variation (CV) associated with the length estimates was 5.1% (Gordon, 1990). This technique was also employed by Christal and Whitehead (1997) in the breeding grounds off the Galapagos Islands, but only two males were measured and were estimated to be 12.33 and 16.27 metres long. Other studies aboard aircraft have used a fixed focal length still camera with range to the whale being measured using an altimeter. Armed with this information the whale's body length can be measured as a proportion of the field of view of the photo. This aerial technique has been used to estimate the lengths of bowhead whales (Ray et al., 1984; Angliss et al., 1995; Perryman and Lynn, 2002), right whales (Best and Ruther, 1992), blue and humpback whales (Calambokidis et al., 1989), fin whales (Ratnaswamy and Winn, 1993) and beluga whales (Ray et al., 1984).

Jaquet (2006) used a laser rangefinder while taking photo-ID shots of flukes, in order to measure fluke width. From whaling data she developed a regression relationship between fluke width and total length, and so was able to estimate total length from this simple technique. Approaches which measure the blowhole to dorsal fin distance (e.g. Gordon, 1991; Dawson et al., 1995) should be inherently more accurate as the distance measured is in the same plane as total length, and indeed accounts for nearly two-thirds of it.

Stereo photography allows reconstruction of a 3-dimensional (3D) image, enabling accurate measurements to be taken in 3-D. Almost all systems consist of two cameras mounted at a known distance apart with parallel overlapping fields of view. The photos are taken simultaneously and are analysed as a pair. Cubbage and Calambokidis (1987) used an aerial stereo system to measure bowhead whales in the arctic. They obtained a CV for objects of

known size of 1.7%. Dawson et al. (1995) and Rhinelander and Dawson (2004) used a stereo system which was boat based to measure sperm whales off Kaikoura. Mean CVs of whales measured multiple times were 4.35% and 3.1% respectively. One obvious reason why CVs are larger is that they relate not to inanimate objects used for calibration but to actual whales, which are inherently flexible (Dawson et al., 1995). Past studies have used an analog stereo-plotter to analyse the stereo pairs but, with the improvement in computing power, analytical photogrammetry software is now available (Mikhail et al., 2001).

Depending on the research platform used (i.e. boat or aeroplane) there are associated limitations. Length estimates taken from an aeroplane do not usually allow repeated measurements of known individuals. This is because identification of individuals normally requires photo-identification from water level (*i.e.* aboard boats). Boat-based measurements however allow for individual identification and recapture by photo-ID. This allows estimates of growth rates and the size frequency of the population (Rhinelander, 2001). The one drawback from boat-based measurements is that they can only measure a portion of the animal's body. For sperm whales this is the blowhole to the dorsal fin. Consequently total length must be calculated from body proportion measurements from whaling records. This leads to increased error, and there are documented cases of a whale's length being overestimated deliberately for individuals that were near legal minimum size (Cooke et al., 1983).

1.10 Thesis objectives

This thesis has three main objectives;

1) To develop a new boat based digital stereo photogrammetry system and assess its measurement accuracy (Chapter 2).

2) Improve the relationship between IPI and total length via increasing the sample size of measured whales, and via applying improved photogrammetric and acoustic analysis methods (Chapter 3).

3) Acoustically estimate growth rates of seasonal resident sperm whales that have been recorded multiple times at Kaikoura (Chapter 4).

1.11 Thesis outline

Each main body chapter (Chapter; 2, 3, 4) is formatted as a standalone paper that is going to be submitted for publication. This fact results in some repetition among chapters. This has been reduced by providing a general introduction and a general discussion and by combining all references in one list at the end of this thesis.

Due to the long-term nature of the dataset many researchers have collected the data that I have had the privilege of analysing. In saying that, I undertook all the data collection, analyses and writing for chapters 2 and 3.

Chapter 4 is co-authored with PhD candidate Brian Miller and expands upon work from his thesis. Brian wrote the majority of the manuscript, fitted the growth curves and developed the IPI plugin. I collected three field seasons worth of data, digitised all the Uhër recordings, computed all the IPIs from all the archived recordings, supplied the latest IPI vs. total length equation and described the digitising process of the Uhër tapes.

Chapter 2: Development of a digital stereo photogrammetric system to measure cetaceans at sea[2]

2.1 Abstract

A new boat-based fully digital stereo photogrammetric system has been developed, calibrated, and had its measurement accuracy assessed for the purpose of remotely measuring free ranging sperm whales. The system was self-calibrated using the close-range photogrammetric software *Australis* (version 6.01, Photometrix Pty Ltd, Australia). To test the accuracy of the calibration values; paired stereo images were used to measure objects of known length in two experiments designed to simulate potential sources of error in the field. In each, conjugate points in the images were measured via two methods; 1) using an automated centroid detection method; 2) a manual measurement method, which replicated the procedure which would occur in the field. The first experiment tested the effect of worsening geometry between the target and the stereo system on measurement accuracy. The second experiment tested the stability of the camera mounting system by assessing measurement accuracy during repeated removal and reattachment of the cameras. Over both experiments the automatic measurement method was more accurate due to its ability to achieve sub-pixel detection of the centre of circular targets. The mean measurement error over the entire distance/angle network for the automatic measurement method was 0.4% (range = 0-1.71%) compared to 0.82% (range = 0.01-4.73%) for the manual measurement method. Manual selection of conjugate points was less accurate as user interpretation introduces variability in selecting the conjugate image points, but is necessary with whale targets. Over the range of distances and angles deemed acceptable for measuring whales (i.e. 40-60m range; angle $<20^{o}$ from parallel to the target), mean error (manual selection) of whale sized targets was 0.74% (range = 0.01-4.5%). The second experiment showed that remounting the two cameras on the stereo bar contributed significantly to measurement error. This is because the exterior orientation values depart from those obtained during indoor calibration. Nevertheless, the error associated with imperfect repeatability of camera orientation is about the same as that associated with manually selecting the measurement points in the conjugate images. Measurement error is acceptably small (< 4%) considering that the targets (sperm whales) are themselves inherently flexible.

---

[1] Growcott, A. Sirguey, P. and Dawson, S (in prep) Development of a digital stereo photogrammetry system to measure cetaceans at sea.

2.2 Introduction

In the context of collecting ecological data, photogrammetry has proven to be a useful technique to estimate remotely the size of free-ranging cetacean species (Dawson et al., 1995; Perryman and Westlake, 1998; Perryman and Lynn, 2002; Jaquet, 2006). Knowing the length of individuals can allow information such as the identification of gender, age, or level of physical/sexual maturity to be inferred (Dawson et al. 1995; Rhinelander and Dawson, 2004; Jaquet, 2006). In the case of exploited and/or endangered species, such information could be valuable in determining the health of the population in question.

Three main photogrammetric techniques have been developed to estimate the size of individuals from one or more photographs captured in the field. First, a single image can be used in which an object of known size is visible at the same distance as the individual to provide a scale (e.g. Durban and Parsons, 2006). Alternatively, the size of the individual can be estimated from a single image along with a range measurement (e.g. Perryman and Lynn, 1993). Finally, stereo images from two cameras enable space intersection to be computed between conjugate image points. Thus, the 3-dimensional (3-D) coordinates of points that are visible in each image forming the stereo pair can be found in object space and distances between them can be determined.

In the context of measuring cetacean size with photogrammetric techniques, studies have used single and stereo imaging protocols. For example, Rowe and Dawson (2008) projected parallel laser beams with a known baseline onto the dorsal fin of bottlenose dolphins while taking photographs. Thus, the laser dots visible in the photos at a known distance apart provided a scale allowing the size of the fin to be determined. Perryman and Lynn (2002) captured vertical aerial photographs of grey whales using a reconnaissance camera with a fixed focal length. A radar altimeter provided the range to the whale, thus permitting whale sizes to be estimated. With two or more overlapping images, close-range photogrammetric techniques take advantage of the multiple vantage points to allow reconstruction of a 3-D model of the object via space intersection of conjugate light rays. For moving targets in wildlife studies, the images must be captured simultaneously. Thus, conventional stereo systems often consist of two cameras mounted onto a rigid body. The latter provides a fixed and known baseline while images from each camera are captured with overlapping field of views. This technique has been used successfully to measure Hector's dolphins (Bräger and Chong, 1999), bottlenose dolphins (Chong and Schneider 2001), bowhead whales (Cubbage

and Calambokidis, 1987), fin whales (Ratnasany and Winn, 1993), and sperm whales (Dawson et al. 1995; Rhinelander and Dawson, 2004).

In the context of sperm whales, four studies have involved boat-based photogrammetry to estimate length. From a known height up the mast of his research vessel, Gordon (1990) took photographs of whales at the surface while they were parallel to the boat. The angle between the horizon and the whale was measured on the developed film and the range was estimated from the curvature of the earth. Jaquet (2006) measured the fluke width of diving sperm whale from digital images which had accompanying range data from a laser rangefinder. She then estimated total length from fluke width via a regression relationship calculated from whaling and stranding data. Dawson et al. (1995) and Rhinelander and Dawson (2004) used a boat-based stereo camera system to measure the distance between the blowhole and posterior emargination of the dorsal fin of sperm whales at Kaikoura, New Zealand. Two non-metric film cameras were attached to an aluminum bar to maintain a constant base separation and activated via a paired air release. The total length was then obtained from body proportion measurements derived from whaling records.

The relatively simple system developed by Dawson et al. (1995) and subsequently used by Rhinelander and Dawson (2004) was found particularly competitive for measuring the whale's total length. Indeed, the mean coefficients of variation (CV) for both studies were 4.4% and 3.1%, respectively. This was substantially smaller than the CV of 5.1% obtained by Gordon's (1990). Jaquet (2006), however, obtained a CV of 1.3% based on repeat measurements of fluke width. Nevertheless, the method used by Jaquet (2006) is more prone to error in extrapolation to total length, because the relationship between the total length and fluke width is much weaker ($r^2 = 0.87$; Jaquet, 2006) than the relationship between blow-hole to dorsal fin and total length ($r^2 = 0.97$; Best, 1990). For this reason, the general approach of Dawson et al. (1995) appears more desirable. It has the potential to provide a simple and accurate way to measure the length of sperm whales using a boat as a research platform.

Nevertheless, the actual system designed by Dawson et al (1995) had several flaws and is impractical today. It was film-based, and relied on the availability of an analog stereo plotter, which is a complex, expensive and now obsolete piece of equipment. In order to obtain a measurement from each stereo pair, the exterior orientation of the two frames had to be determined empirically. Thus, the cost, technical knowledge, and time requirement needed to use and implement stereo photogrammetry limited its application by other researchers.

The measurement accuracy of this analog system was compromised by an incomplete internal calibration procedure in which only the focal length of each lens was measured. Additional internal orientation parameters such as the position of the principal point of autocollimation (PPA) with respect to the center of the frame and the lens radial distortion were ignored. These parameters are important for modelling the space intersection of light rays originating from conjugate points identified in each frame of a stereo pair (Mikhail et al., 2001, Chap. 3). Despite satisfactory overall performance, Dawson et al. (1995) showed that the accuracy of the system decreased substantially as the angle between the optical axis of the cameras and the object photographed departed from a right angle. Although this effect was predictable due to the loss of ideal geometry between the stereo system and the object, its severity could be partly attributed to the limited internal calibration of the cameras. Other limitations were that the shutter activation of the two cameras was at times asynchronous, and the need to manually advance the films limited the number of stereo pairs that could be captured per encounter.

Progress in digital camera and computer technology now enables close range photogrammetry problem to be fully digital (Mikhail et al., 2001). Analytical processing, whereby a fully deterministic mathematical solution is found for the photogrammetric problem, can now be readily implemented with standard off-the-shelf digital cameras. This enables many of the shortcomings associated with the analog stereo system and analog processing to be overcome. This study reports on the design of a new digital stereo photogrammetric system for measurement of sperm whales, its calibration, and accuracy assessment.

2.3 Methods

2.3.1 Digital stereo camera system

The stereo photogrammetric system designed in this study is a modification of that designed by Dawson et al. (1995). The original analog film cameras and air release trigger have been replaced by two Nikon D70s single-lens reflex (SLR) digital cameras equipped with AF Nikkor 50mm f/1.8D lenses and a custom-built electronic remote trigger. The lenses were set to manual focus, and their focussing rings taped in place at infinity focus to maintain a constant interior orientation. The cameras were set to 400 ISO, shutter priority automatic exposure, with shutter speeds fixed at $1/1250^{th}$ of a second to minimise motion blur. In the field, natural light was sufficient to ensure that images were sharp from 30m to infinity. The stereo bar and eye-height mast to which it was attached were adapted from the previous system described by Dawson et al. (1995).

In the context of photogrammetry, several parameters must be determined to measure accurately the length of objects from stereo photographs. One set of parameters known as interior orientation relates to the geometrical properties of the lens. They involve the precise focal length, the position of the PPA with respect to the centre of frame, and the radial/tangential distortion profile of the lens. The other parameters, known as exterior orientation, summarise the precise position and orientation of the cameras to each other (Mikhail et al., 2001). Thus, the exterior orientation is defined by six parameters:

1. Three parameters describing the position of each camera (x,y,z);
2. Three parameters describing the orientation of each camera (azimuth, elevation, roll).

These parameters can be estimated by performing an indoor calibration procedure using close range photogrammetric software. A diagram of the digital stereo camera configuration is shown in Fig 2.1.

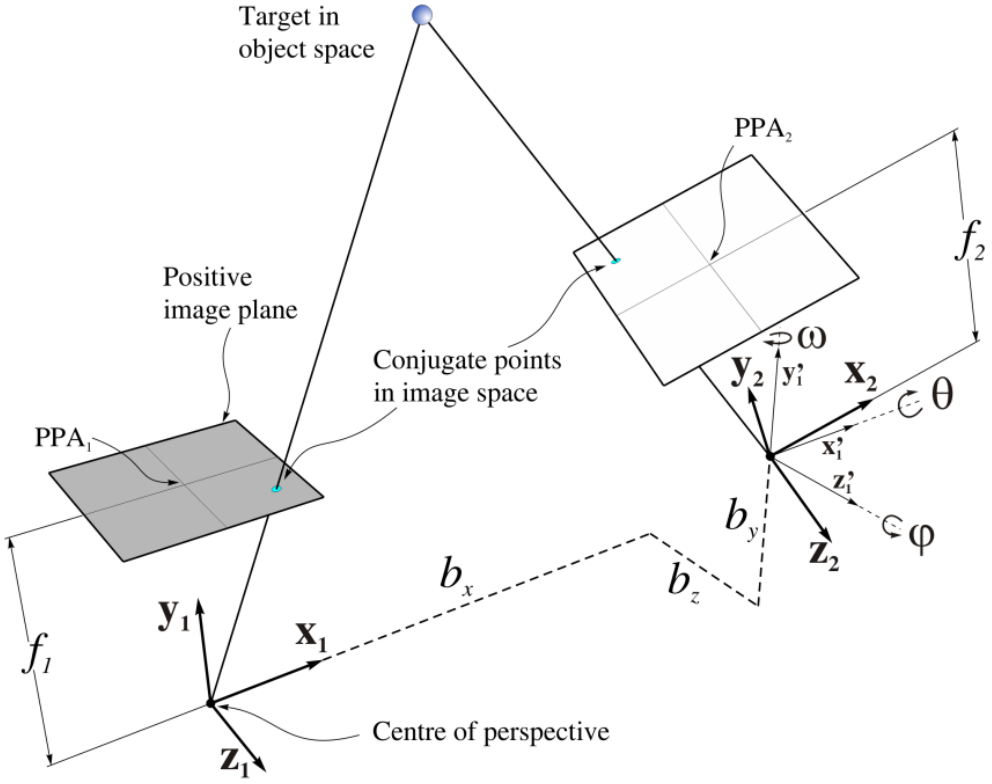

Figure 2.1 Geometry of the stereo camera system. ($\mathbf{x_1}$, $\mathbf{y_1}$, $\mathbf{z_1}$) and ($\mathbf{x_2}$, $\mathbf{y_2}$, $\mathbf{z_2}$) are the coordinate system attached to the left (camera one) and right (camera two) camera, respectively. b_x, b_y, and b_z represent the three translations from the coordinate system of camera 1 to that of camera 2. ($\mathbf{x_2}$, $\mathbf{y_2}$, $\mathbf{z_2}$) are obtained via three sequential rotations (positive rotation of angle φ around the z axis; positive rotation of angle θ around the x axis, and negative rotation of angle ω around the y axis). PPA and *f* denote the principal point of auto-collimation and focal length of each camera, thus representing the main parameters of interior orientation.

2.3.2 Calibration using *Australis*

The close range photogrammetric software *Australis* (version 6.01, Photometrix Pty Ltd, Australia) was used for the calibration of the cameras (i.e., to determine the interior orientation of each camera, as well as the exterior orientation of one camera with respect to the other). *Australis* can also be used to measure the positions and dimensions of objects identified in the stereo pairs.

A self-calibration strategy was chosen whereby many images of a calibration wall were captured by each camera from various vantage points and orientations. The calibration wall consisted of reference targets whose positions are precisely known. The targets were white circular reflective surfaces on a black background. *Australis* has the capability of locating and

labelling automatically the centroid of such round and high contrasted targets. This feature enables measurements of points to be obtained at sub-pixel level with high accuracy, thus ensuring the accurate determination of internal and external orientation parameters.

The internal orientation parameters as well as the external orientation for each single image were then computed in *Australis* by means of a bundle block adjustment. This process estimates simultaneously all unknown parameters using an iterative least squares solution of the linearised form of the co-linearity equations (Mikhail et al., 2001, Chap. 9). Figure 2.2 illustrates the exposure stations of 14 images of the calibration wall determined after bundle block adjustment.

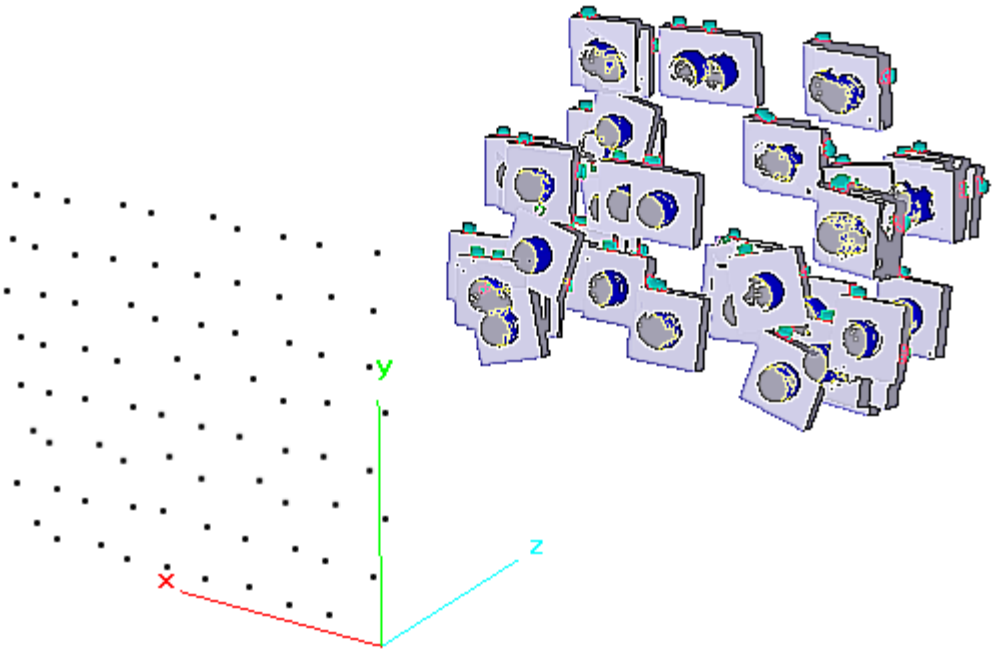

Figure 2.2 The 3-dimensional model of the calibration wall along with the reconstructed positions of cameras obtained via the bundle block adjustment.

The *Australis* software is limited in the sense that it cannot readily accommodate a stereo configuration. In other words, the exterior orientation parameters are determined with respect to a reference system attached to the calibration wall under the assumption that all individual images are independent. In order to retrieve measurements from stereo pairs captured with two cameras mounted on a rigid body, it is necessary to determine the exterior orientation of one camera (e.g., the right camera) with respect to the other (e.g., the left camera). Only then can a space intersection be processed to locate a point in object space (i.e., 3-D coordinates)

from the positive identification of the two conjugate image points visible in the images forming the stereo pair (see Fig 2.1).

Once the exterior orientation of two images is determined with respect to the calibration wall by means of bundle block adjustment, it becomes relatively simple to reduce the position and orientation of each frame so that a new origin is set on the perspective centre of the left camera. This is achieved by transforming the coordinates from camera 2 to the wall, and subsequently from the wall to camera 1. A new rotation matrix and translation vector are determined based on the exterior orientation of each frame as explained in the Appendix .

The calibration process was completed by first capturing 20 photos of the calibration wall with each camera. Each of these 20 photos was captured from a different position. The calibration wall was photographed from various distances and angles to enable a robust estimation of the parameters. Then, each camera was attached to the stereo bar and seven stereo pairs of the calibration wall were captured with the system placed at different positions and angles. The cameras were then taken off the stereo bar and remounted to capture another set of seven stereo pairs. This procedure was repeated to obtain three independent sets of seven stereo pairs. The purpose of this protocol was to investigate the robustness of the exterior orientation enforced by the bar with respect to mounting and dismounting the cameras. Thus, this procedure simulated the fact that, each day on the boat, the cameras are mounted on the bar once on site and removed before going back to shore.

A limited number of stereo pairs were taken due to the length of the stereo bar (i.e., 2.5m) being relatively large compared to the calibration room. The additional 20 images captured independently by each stand alone camera provided the redundancy required to allow a more accurate determination of the internal orientation parameters of the lens. The final exterior orientation parameters of the stereo system (i.e., the translation vector and rotation matrix of the right camera with respect to the left) were obtained by averaging the corresponding values obtained from the three sets of seven stereo pairs.

2.3.3 Field testing of the calibrated digital stereo system

In order to assess the robustness and accuracy of the calibrated stereo system, a field experiment was conducted. The experiment had four main purposes.

1) To test whether the calibration of the digital stereo system obtained indoor allows accurate measurements in the field.

2) To investigate the effect of the relative angle and distance between the stereo system and the target in order to assess how the geometrical setting affected measurement accuracy.

3) To assess how dismounting and remounting the cameras onto the bar affected measurement accuracy.

4) To assess how the manual measurement of conjugate points on the stereo pairs, as interpreted by a user, affected accuracy.

The experiment was conducted on a sports field. In order to replicate exactly how sperm whales would be measured in real conditions, five images of a blowhole and five of a dorsal fin printed at life-size were attached to a fence at five different distances [4, 6, 8, 10, and 12 metres apart. Note that the distance between the blowhole and dorsal fin from whales measured at Kaikoura is approximately 7.5-10 metres (Dawson et al., 1995; Rhinelander and Dawson, 2004)]. The measured distances were chosen to encompass the likely whale size that this project would encounter. Directly beneath each of these photographs, a white circle of 10 cm in diameter was taped onto a black background to enable automatic point measurement in *Australis*.

A network consisting of four distances from the fence (40, 50, 60, 70 metres) and seven angles (-30, -20, -10, 0, 10, 20, 30 degrees) (see Fig 2.3) was constructed using a total station (Nikon NPL-362) and a corner reflector. Each position once found was marked in the ground with a wooden peg. Within this framework two separate experiments were conducted:

1. first, one stereo pair was captured at each of the 28 locations to test the effect that distance and angle between the system and the target had on measurement error;

2. second, 10 stereo pairs were taken at three positions of the network, with the cameras being dismounted then re-mounted on the stereo bar between each exposition. This second experiment aimed at quantifying the error associated with removing and remounting the cameras on the stereo bar. The three positions in the network were chosen to represent the worst geometry whereby the parallax is minimised (-30°, 70

m), the best geometry whereby the parallax is maximised (0°, 40m), and an intermediate geometry at close distance but severe angle (-30°, 40m).

For each experiment, two methods of measurement were conducted in *Australis*. First, the automatic centroid detection feature available in *Australis* was used to determine automatically the position of the centre of the white circle with sub-pixel accuracy. This method allowed the stereo system to be tested in terms of its absolute accuracy, without the user potentially introducing uncertainties and bias when interpreting the position of conjugate points in the stereo pairs. Second, the user measured manually the conjugate locations of the blowhole and the dorsal fin printed on the boards to enable the assessment of human error. Each measurement was repeated three times to allow calculation of variance.

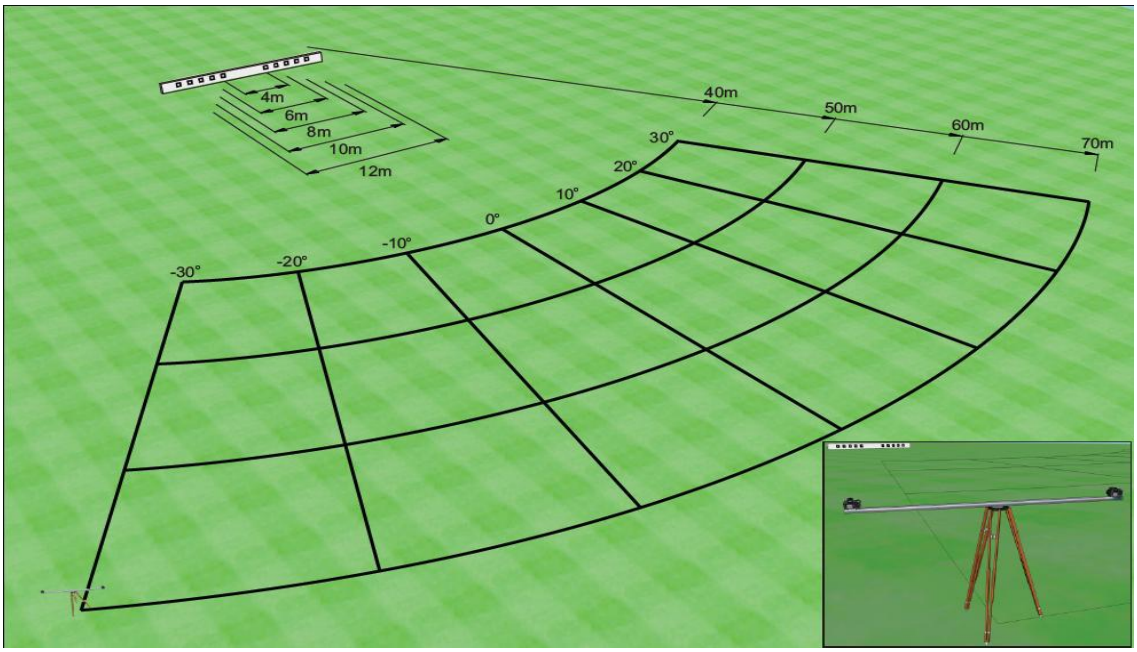

Figure 2.3 The assessment network showing the four distances (40, 50, 60, 70 metres) and seven angles (-30, -20, -10, 0, 10, 20, 30 degrees) from where the stereo pairs were captured, as well as the measured distances (4, 6, 8, 10, 12 metres). Image courtesy of Dr. Pascal Sirguey.

2.4 Results

The averaged values and standard deviation of the exterior orientation parameters relative to the right and left camera obtained during indoor calibration are shown in Table 1. The relative error of measurement over the entire network is shown for automatic and manual

measurement methods for two measured lengths, 8 metres and 10 metres (Fig 2.4). The automatic measurement method over all the measured distances is less variable (mean error = 0.4%, range = 0-1.71%), than the manual method (mean error = 0.82%, range = 0.01-4.73%) because it involves a deterministic and therefore repeatable technique. Only two measured distances are shown because the pattern was similar over all other measured distances.

Table 2.1 Average value and standard deviation of the exterior orientation parameters between the left camera (used as origin) and right camera, rounded to 3 decimal places.

	b_x [mm]	**b_y [mm]**	**b_z [mm]**	**φ [deg]**	**θ [deg]**	**ω [deg]**
Mean	2398.041	11.402	-2.647	0.424	0.726	-0.145
Standard deviation	2.601	0.948	2.643	0.019	0.029	0.080

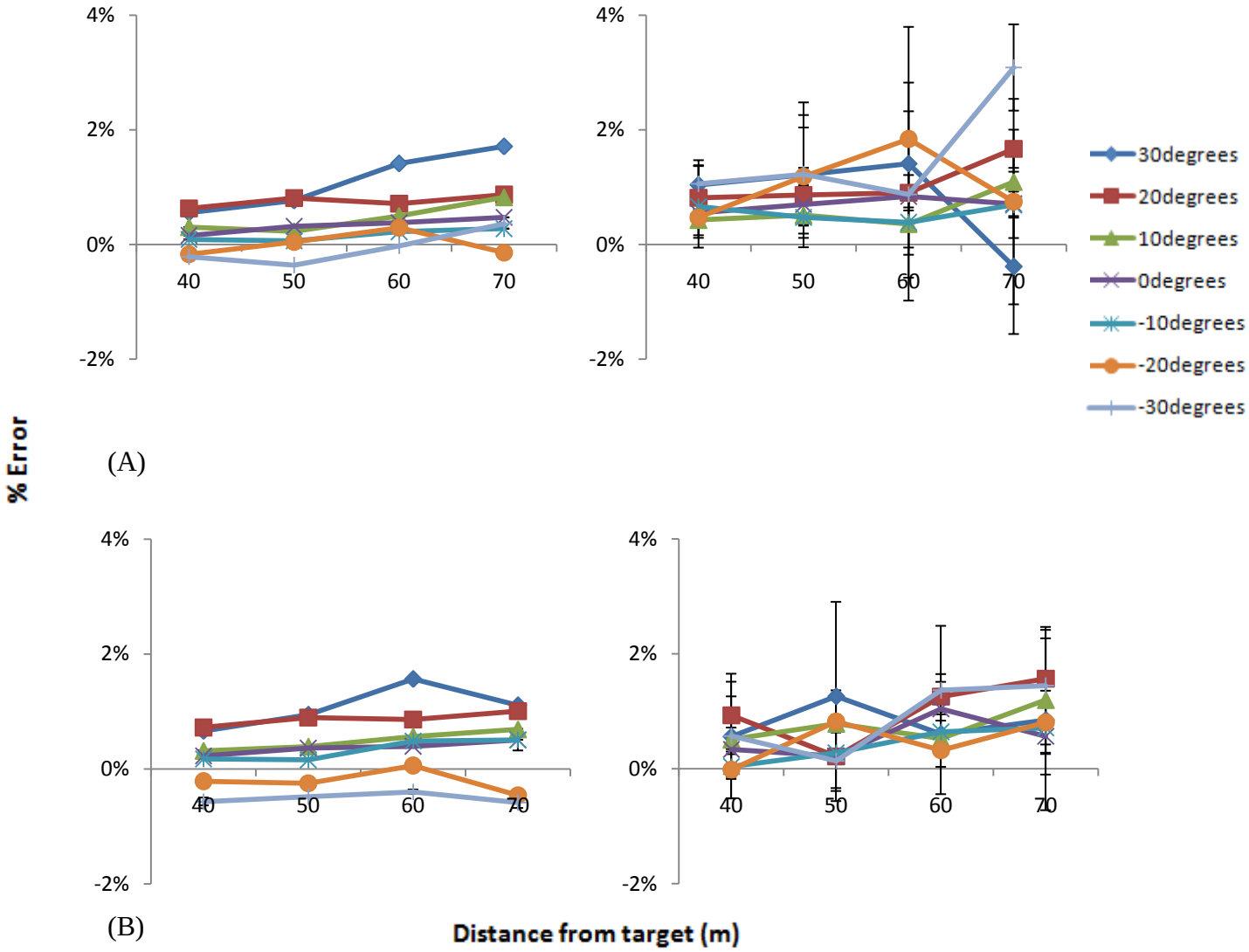

Figure 2.4 Relative errors for automatic (left) and manual (right) measurement methods when measuring a length of a) 8 metres and b) 10 metres, over the whole network. The error bars represent ± one standard deviation. The key shows at which angle the stereo pairs were captured.

A general linear model showed that the variance in the measurements is significantly influenced by a number of factors (Table 2.2). The factor explaining most of the variance of the error was the measurement method used (F-value=81.52, $p<0.001$). The angle at which the photo was captured came second (F-value=20.99, $p<0.001$), followed by the interaction effect between the measurement method and the angle error (F-value=13.26, $p<0.001$).

Finally, the distance between the system and the target also explained a significant amount of measurement errors ($F=10.51$, $p<0.001$).

Table 2.2 Results of the general linear model for the distance/angle field experiment. Sources of error are arranged by F-values (Highest to lowest). D.F = Degrees of freedom.

Source	D.F	F-value	P-value
Method	1	81.52	<0.001
Angle	6	20.99	<0.001
Method*angle	6	13.26	<0.001
Distance	3	10.51	<0.001
Wall distance	4	7.08	<0.001
Wall distance*method	4	2.87	0.029
Wall distance*angle	24	2.47	0.002
Wall*method*angle	24	2.44	0.002
Angle*distance	18	2.01	0.020
Method*angle*distance	18	1.78	0.045
Wall distance*method*distance	12	1.09	0.385
Wall distance*angle*distance	72	1.08	0.379
Wall distance*distance	12	0.99	0.463
Method*distance	3	0.2	0.896

From the second experiment, the relative error associated with the remounting of the two cameras between expositions is shown in Fig 2.5. The mean error when investigating the manual selection of conjugate points was lowest at intermediate geometry (40 metres, 30 degrees), highest at the worst geometry (70 metres, 0 degrees) and medium at the best geometry (40 metres, 0 degrees) and were 0.64% (range = 0.02-2.49%), 0.66% (range = 0.02-1.58%), and, 1.08% (range = 0.18-4.5%), respectively.

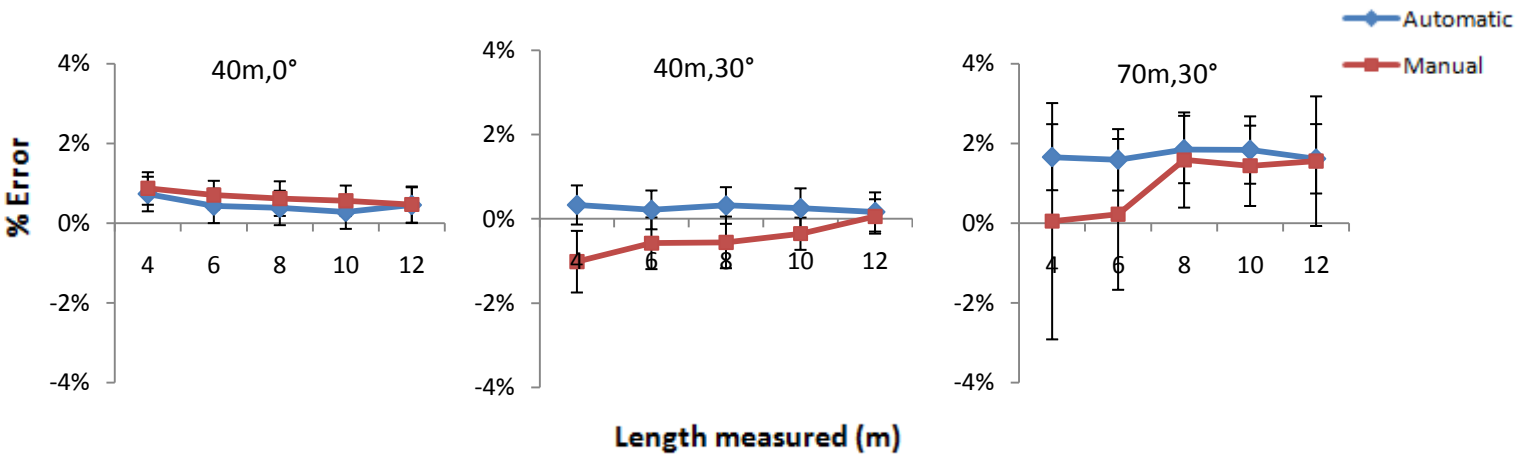

Figure 2.5 Relative error for the experiment that involved remounting the cameras between each exposition (10 replications for each position). Two measurement methods are compared (i.e., automatic and manual). The stereo pairs processed for the left, middle, and right graphs were captured from positions 40 metres - 0 degrees, 40 metres - 30 degrees, 70 metres - 30 degrees, respectively. The error bars represents ± one standard deviation.

Again, a general linear model was used to identify the sources which contributed the most to variance of the measurement error (Table 2.3). The variance in the measurements was significantly influenced by three factors. The position at which the stereo pairs were captured appeared to explain most of the variance (F-value=62.72, $p<0.001$). The method used to measure the photographs came second (F-value=16.57, $p<0.001$). Finally, the interaction between position and method came third (F-value=8.54, $p<0.001$).

Table 2.3 Results from the general linear model for the re-mounting experiment. The sources of error are arranged by F-value. D.F = Degrees of freedom.

Source	D.F	F-value	P-value
Position	2	62.72	<0.001
Method	1	16.57	<0.001
Position*Method	2	8.54	<0.001
Wall distance*Method	4	2.2	0.07
Position*Wall distance	8	1.98	0.049
Wall distance	4	1.48	0.208
Position*Wall distance*Method	8	0.98	0.449

Because the two experiments were conducted independently, it was not readily possible to discriminate whether the relative geometry between the stereo system and the target (i.e., the distance and angle at which the picture was captured) or the process of dismounting and remounting the cameras between expositions influenced the error the most. In order to elucidate this question, the relative errors from both experiments obtained with the automatic measurement method were plotted for the corresponding positions (Fig 2.6). It reveals that remounting the cameras introduced more variability in measurements and that this variability increased as the geometry with respect to the target worsens.

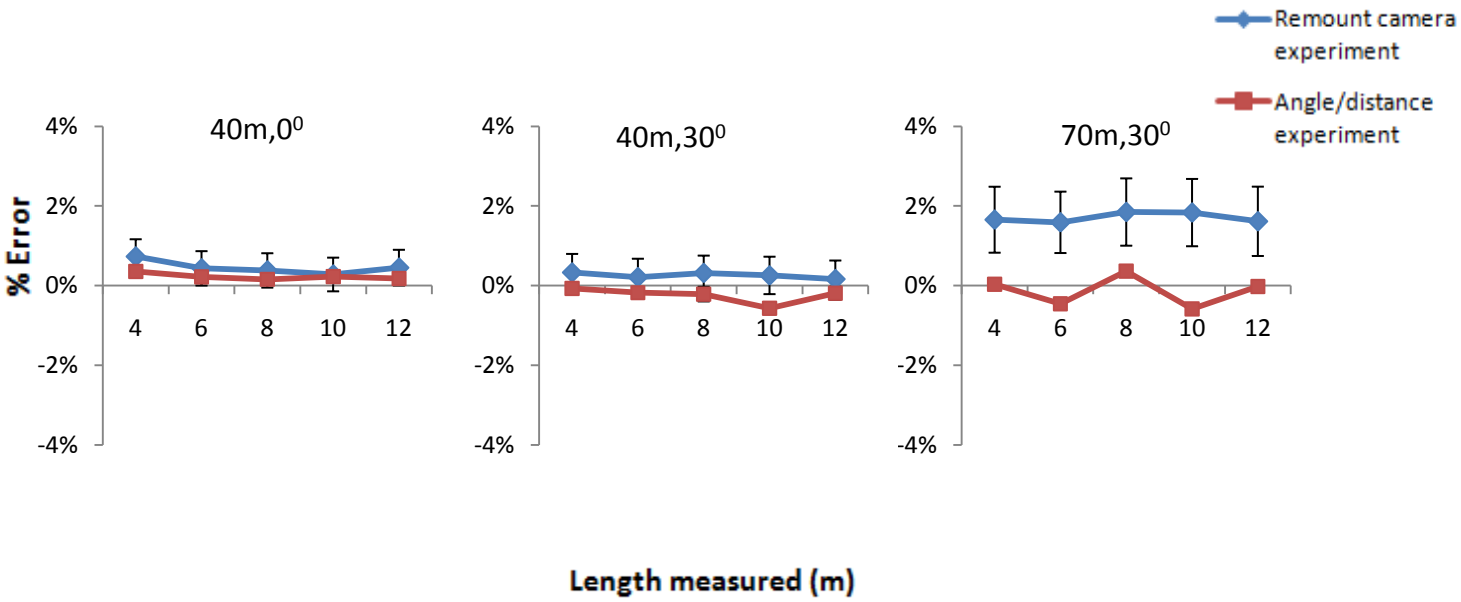

Figure 2.6 Comparison of relative error for the corresponding positions of both experiments (automatic measurement method only). The left, middle, and right graphs correspond to stereo pairs captured at positions 40 metres - 0 degrees, 40 metres - 30 degrees, and 70 metres - 30 degrees. The error bars correspond to ± one standard deviation.

When using the digital stereo system in the field to measure sperm whales, only the manual measurement method can be used. Thus, both experiments were also compared with respect to distances obtained from manual measurements. Figure 2.7 demonstrates that there is a considerable overlap in error bars for all but one measured distance.

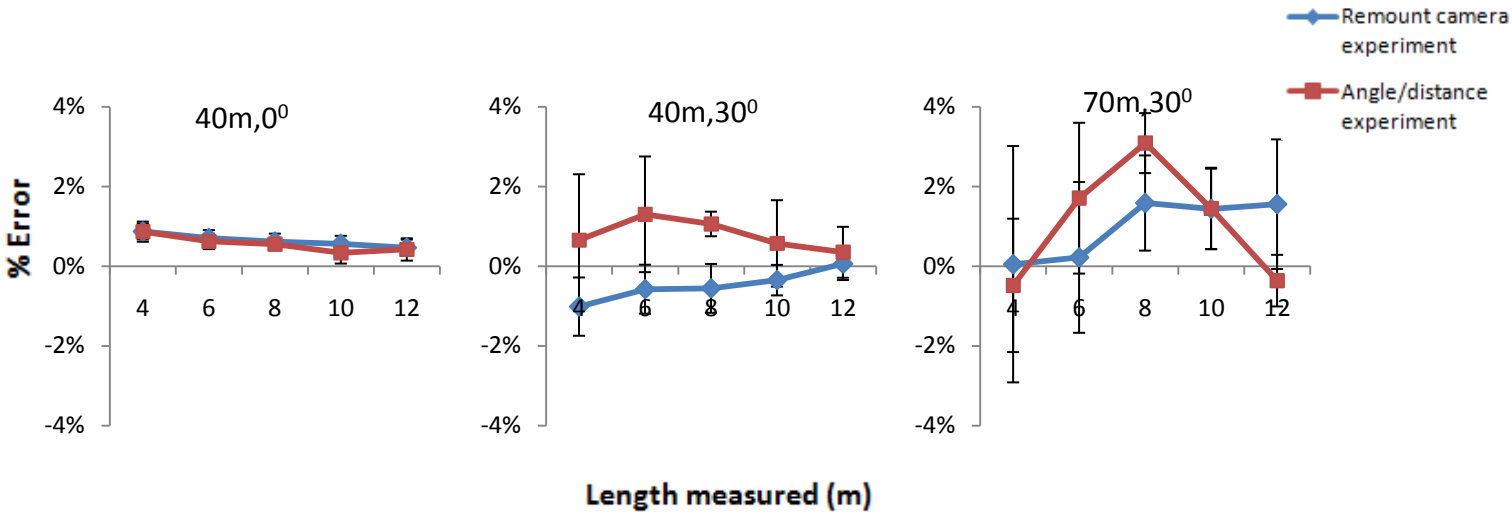

Figure 2.7 Comparison of relative error for the corresponding positions of both experiments (manual measurement method only). The left, middle, and right graphs correspond to stereo pairs captured at positions 40 metres - 0 degrees, 40 metres - 30 degrees, and 70 metres - 30 degrees. The error bars correspond to ± one standard deviation.

2.5 Discussion

A digital stereo camera system has been developed, calibrated, and had its accuracy assessed for the purpose of measuring sperm whales at sea.

The indoor calibration of the digital stereo system facilitated the estimation of both the interior and exterior orientation parameters. To test the stability of the exterior orientation values, three sets of seven stereo pairs were captured, with the cameras being removed and remounted between each set. The standard deviation associated with each exterior parameter was small. Therefore, they were considered valid for use.

To further examine the suitability of the exterior orientation parameters an outdoor experiment was conducted. This included measuring a range of targets of known length, in a protocol that replicated what would occur in the field. The first experiment tested the effect of geometry and the subjective interpretation of conjugate points on measurement accuracy. The angle and distance at which stereo pairs were captured explained a significant amount of measurement uncertainty. Nevertheless, the manual selection of conjugate points in the stereo pairs appeared to contribute more to measurement uncertainty. The automatic measurement method is able to locate the centroid of high contrast circles to sub-pixel accuracy. Therefore, there is minimal variation between repeated measurements of the same stereo pair.

Alternatively, the manual selection of conjugate points is influenced by human interpretation, which inherently compromises the repeatability of the process (Dawson et al., 1995).

The second experiment tested the effect that removing and remounting the cameras had on measurement error. As mentioned earlier, the exterior orientation values were replicated during the indoor calibration process and found to be relatively stable. Nevertheless, it remains important to test how this inherent variability would affect measurements in the field. This remounting procedure was tested over three positions (40 metres - 0 degrees, 40 metres - 30 degrees, and 70 metres - 30 degrees). In the first hand, the differing positions explained most of the measurement uncertainty. This can be explained by the fact that, as the geometry between the stereo system and the target worsens (i.e., distance and/or absolute angle increasing) so would the parallax, resulting in a decrease in measurement accuracy. In light of this, the mean measurement error is lowest for the intermediate position (40 metres – 30 degrees). However, the range of measurement errors is smallest for the position with the ideal geometry (40 metres – 0 degrees). In addition, at further distance the spatial resolution gets coarser, thus complicating the measurement of conjugate points. On the other hand, the manual selection of conjugate points also explained a significant proportion of measurement uncertainty.

While we did not combine these factors in an experiment, an assessment of the relative contribution of errors resulting from the geometry of the system to the target vs mounting and remounting the cameras is possible from comparing the standard deviations associated with each. It appears that the error associated with the manual identification of the blowhole and posterior emargination of the dorsal fin (i.e., the user error) is comparable to that associated the process of remounting the cameras on the stereo bar between trials. Thus, the exterior orientation parameters determined during the indoor calibration of the system are confirmed to be robust enough for accurate measurements. Moreover, the process of visual interpretation of conjugate points and remounting of the cameras are independent. Therefore, the error associated with the first process has no effect on that introduced by the other. Recalibration of the stereo system after remounting the cameras is unnecessary given that the user interpretation of conjugate points will introduce at least as much uncertainty.

The advantage of using two different measurement methods is that the automatic method permitted a deterministic and repeatable measurement of conjugate points, which enables the system to be consistently assessed, while the manual measurement accounts for user bias and interpretation. However, in the field it is only possible to use the manual measurement

method. These two experiments have allowed the two measurement methods to be assessed independently. This provided an objective way to quantify the effect that manually selecting conjugate points in the stereo pairs has on measurement error.

It also must be kept in mind that another factor limiting the accuracy of measurements is that sperm whales are inherently flexible (Dawson et al., 1995). Therefore, it is believed that a more accurate system will not necessarily result in a more precise estimate of whale length.

This new digital stereo system has eliminated many of the shortcomings of the previously used analog system. Further, its measurements of individual whales are much more consistent. Repeated measurements of the same whale at sea show a mean C.V of 1.57% (Chapter 3). For the old, analog system this figure was almost three times larger (CV = 4.35%: Dawson et al., 1995). The only specialised item required to design a similar system is the photogrammetry software *Australis* or any alternative but equivalent package (e.g., Photomodeller). This new system proved to be simple to calibrate and to use, while providing a simpler and more accurate way to measure the distance between the blowhole and posterior emargination of the dorsal fin of sperm whales. Close-range photogrammetry software such as *Australis* is also very flexible in that a variety of camera sensors and lenses can be calibrated and used to suit the intended application. If designing a similar system for either biological or non-biological purposes, it is expected that the accuracy would be further improved by keeping the cameras permanently mounted on the stereo bar.

Chapter 3: Measuring whales from their clicks: a new relationship[2]

3.1 Abstract

The most common vocalisations heard from sperm whales are short, broadband clicks which often display a decaying, evenly spaced, multi-pulse structure. The time between these pulses (inter-pulse interval: IPI) represents the two-way time for a pulse to travel between the air sacs located at either end of the sperm whale's head. The IPI therefore, is a measure of head length and due to an allometric relationship, total length. Previous studies relating IPI to an independent measure of length have suffered from very small sample sizes. To address this, sound recordings and digital stereo photogrammetric measurements of 21 individual sperm whales were made off Kaikoura, New Zealand, in order to measure their IPI and total length. In addition, archived recordings were reanalysed. Repeated measurements of the same individuals showed that the stereo photogrammetric system newly built for this task was substantially more accurate than other previously used methods (mean C.V = 1.57%). IPIs were measured via a new software plugin[5] to *Pamguard*, an open-source software package for passive acoustic monitoring. The plug-in was based on the recently developed "bent horn" theory of sound production. IPI measurements were highly consistent within individuals (mean C.V = 0.63%). In part due to improved acoustic and photogrammetric techniques, the equation proposed here relating IPI to total length shows a better fit than any other published for the same purpose.

[2] Growcott, A. Dawson, S. Miller, B. and Sirguey, P. (In prep) Measuring whales from their clicks: a new relationship.

[3]Developed by Miller (2010).

3.2 Introduction

The broadband clicks that are characteristic of sperm whales often display a decaying evenly spaced multi-pulse structure (Backus and Schevill, 1966). The time between these pulses is called the Inter-pulse interval (IPI). Norris and Harvey (1972) first proposed that the IPI is the time for a click to travel backwards from its source (the museau de singe, at the front of the head), along the spermaceti organ to be reflected off the frontal air sac at the front of the skull and travel back along the spermaceti organ to be emitted from the front of the head. The key point is that IPI represents the two-way travel time for click pulses between air sacs located at either end of the whale's head and therefore is a measure of head length. This hypothesis coupled with the allometric relationship between head length and an individual's total length (Nishiwaki et al., 1963) allows remote acoustic size estimation.

Several studies have applied this idea, and computed estimates of total length based on IPI and assumed or measured values for the speed of sound in spermaceti (e.g. Alder-Fenchel, 1980; Goold, 1996). Others have computed IPIs and compared them to visual length estimates (Norris and Harvey, 1972; Amundin, 1978; Mathias et al., 2009), in general showing close correspondence. Without actual measurements of whale length, however, these studies are unconvincing.

The first researcher to develop an empirical relationship between IPI and total length was Gordon (1991). Unlike his predecessors, he had independent measures of the same whale, derived from a simple photogrammetric technique. In doing so he found that Mohl et al.'s (1981) equation gave unrealistically large estimates of total length from IPI; 3-6 meters longer than the photogrammetric estimates. Several problems with this equation were discussed and a new empirically-derived regression based on the 11 acoustically and photogrammetrically measured whales was proposed. While Gordon's approach was refreshingly empirical, his sample was relatively small, and because he was working with nursery groups of sperm whales in the Azores and Sri Lanka, his sample contained mostly females and immatures. Only one animal over 12 metres in length was included. At higher latitudes (>40^{o} N & S) females are very seldom encountered, and most sperm whales are roving "bachelor males" (Rice, 1989), which are up to 50% longer than mature females. For these animals, Gordon's equation might not apply well.

Rhinelander and Dawson (2004) recorded sperm whale vocalisations offshore of Kaikoura, New Zealand and made independent measurements with a boat-based stereo photogrammetric system (Dawson et al., 1995). This was the first study able to make repeated measurements of

the same individuals over time. Within individuals IPIs were stable over short periods, but increased significantly over years, consistent with growth. Their sample size of measured whales (12) included larger whales than had been previously measured (up to 15.3m; as measured via stereo photogrammetry), and they proposed a new regression equation.

All past methods used to measure the IPI of a whale have found that many clicks are unsuitable for analysis as the multi-pulse structure is not always present. Alder-Fenchel (1980), for example, used a ranking system and found that only 11% of analysed clicks fitted the criteria. Rhinelander and Dawson (2004) addressed this problem by confining their analysis to clicks recorded between 2-8 minutes after the whale dived, a time at which the orientation of the whale is such that the multi-pulse structure is generally apparent. Even so, a large proportion of clicks could not be measured.

A recent study has explained why so many clicks display an irregular pulse structure. Mohl et al. (2003) proposed a new "bent horn" model of sound production which is a refinement of the Norris and Harvey (1972) hypothesis (see chapter 1). Zimmer et al. (2005[b]) supported this new model by showing that the orientation of the vocalising whale to that of the hydrophone influences the structure of the click. Clicks recorded on-axis, either behind or in front of the whale display a regular multi-pulsed structure whereas clicks recorded off-axis have a transient pulse which is aspect dependent and its time delay varies depending on the off-axis angle of the click.

Based on the "bent-horn" model, Teloni et al. (2007) have developed a new method for extracting consistent IPI measurements from recordings in which the whale's orientation is unknown. Their approach averages the cepstrum of a large number of clicks, which, in most recordings, will have been recorded from varying aspects, ranges and depths (Teloni et al., 2007) with respect to the hydrophone. The aspect-dependent IPIs will slowly change throughout the recording, however the whale's "true" IPI will be present in every click, even if it is masked by the other IPIs. By averaging all the click cepstra the aspect-dependent IPIs tend to cancel, while the "true" IPI is reinforced, and is left as an estimator of the whale's spermaceti sac length (Teloni et al., 2007). This method, as employed by Miller (2010) as a plug-in for the open source passive acoustic monitoring software (Pamguard,www.pamguard.org), is automated, runs on a standard Windows laptop, and allows IPIs to be calculated from a much larger sample of clicks than would be feasible to measure manually. Until this development, all previous measurements of IPI, while made using various signal processing methods, where essentially manual, measuring one click at a

time (Gordon, 1991; Goold, 1996; Pavan et al., 2000; Rendell and Whitehead, 2004; Rhinelander and Dawson, 2004; Drouot et al., 2004; Marcoux et al., 2006; Jaquet, 2006).

Advances in camera technology and development of off-the-shelf photogrammetric software have increased the precision, accuracy and ease of use of digital stereo photogrammetry. The stereo camera system used by Rhinelander and Dawson (2004) was based on film cameras and measurement of the stereo images was conducted using an analog stereo plotter (Dawson et al., 1995). Digital cameras and computer software allow this process to be fully digital, which should increase model robustness, as additional parameters are accounted for, and dramatically improve usability. In addition the subjectivity when creating three dimensional models using analog stereo plotters is now eliminated.

The past two studies to empirically relate IPI to an independent, non-acoustic measure of whale's length (Gordon, 1991; Rhinelander and Dawson, 2004) are each based on relatively small sample sizes. If IPI measurements are to accurately measure lengths of sperm whales, the relationship needs to be based on more data. The aim, therefore, of this study is to use the latest acoustic and photogrammetry methodologies to develop a new regression equation based on a larger sample.

3.3 Methods

Data for this project were collected over two 3-4 week field seasons (19 June – 9 July 2009; 14 Nov -9 Dec 2009). This work is a continuation of the Otago University research programme on sperm whales which began in 1990 (Childerhouse et al., 1995). Research was conducted aboard a 6.6 metre offshore rigid hull inflatable boat powered by a 100 hp 4-stroke outboard engine. Almost all field work was within a 10 by 20 nautical mile block located south of the Kaikoura peninsula (Fig 3.1). This area overlies the Kaikoura canyon and depths range from between 50-1500 metres. Data collection was limited to sea states of Beaufort 4 and below.

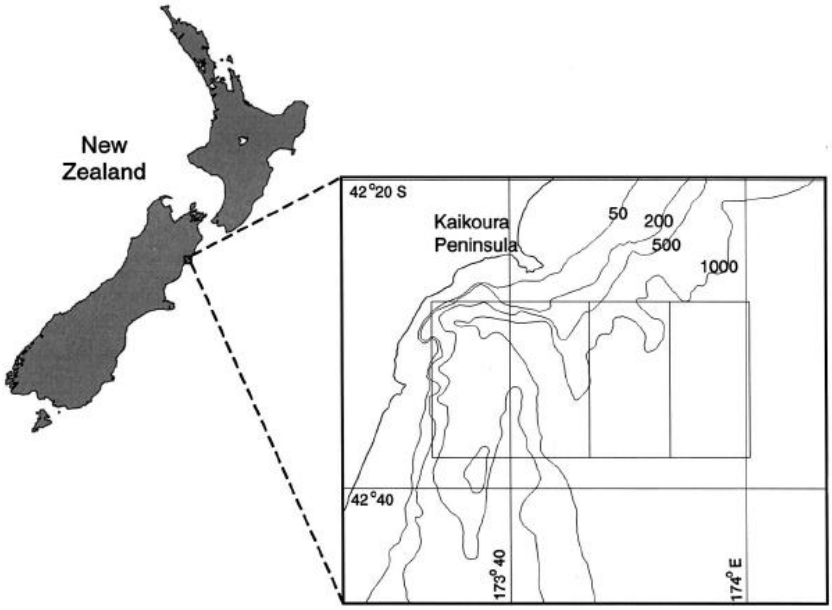

Figure 3.1 Map of New Zealand, showing the bathymetry of the Kaikoura canyon and study site. (from Rhinelander and Dawson, 2004).

Field methodology was based on that of Dawson et al. (1995) and Rhinelander and Dawson (2004). In summary, a custom-built directional hydrophone was used to find and track individual whales. When a whale surfaced the research vessel was gently manoeuvred alongside and the distance between the blowhole and posterior emargination of the dorsal fin measured with a digital stereo photogrammetric system (Chapter 2). Stereo photographs were retained for measurement if they were in-focus, the posterior emargination of the dorsal fin was clearly visible and the angle of the whale relative to the camera system was < 20° off parallel. Each stereo pair was measured three times using the photogrammetry software *Australis* (version 6.01, Photometrix Pty Ltd, Australia) and whale's total length estimated using the regression equation published by Best (1990). Once a sufficient number of stereo photographs were obtained, the boat was manoeuvred behind the whale. A stereo hydrophone array was then deployed (depth of deepest hydrophone either 65 or 105 metres) to record the diving whale's volcalisations and when it fluked an identification (ID) photograph was taken (Arnbom, 1987). ID photographs were shot using either a Nikon D1H or D3 SLR with an AF Nikkor 300mm f2.8 lens or an AF Nikkor 80-200mm f2.8 lens. The target whale was recorded until: a) at least 15 minutes of continuous recording was completed; b) the clicks of the target whale were judged to be too faint or; c) other whales appeared to be closer to the hydrophone array and louder than the target whale. Search effort and sightings were logged via custom written software running on a palmtop computer connected to a GPS navigator. To

assess the stability of camera orientation, at the start of each day an object of known length (2.67 metre floating PVC pipe) was photographed floating in the water.

Sperm whale vocalisations were recorded with a custom-built stereo hydrophone array (Barlow et al., 2008) attached to an Edirol R4 hard drive recorder (sampling at 96 kHz, 16 bit). Archived Digital audio tape (DAT; f_s = 48 kHz, 16 bit) recordings used by Rhinelander and Dawson (2004) had their IPIs re-analysed.

Recordings were analysed using an IPI plugin (Miller, 2010) designed to be used in conjunction with the freely available, open-source passive acoustic monitoring software Pamguard. The IPI plugin employed the IPI estimation method developed by Teloni et al. (2007), using cepstrum analysis (Bogert et al., 1963) to detect the time delay between repeated patterns in a broadband signal. The cepstrum of each click is computed using the equation:

$$Ct = |FFT^{-1} (\log|FFT(x_t)|) \quad (3.1)$$

Where the x_t is the digital recording represented in the time domain. FFT is the fast Fourier transform and FFT^{-1} is the inverse fast Fourier transform (Teloni et al., 2007).

An ensemble average of all the click cepstra is then computed. As explained previously this causes all aspect dependant IPIs to cancel out, thus leaving the 'true' IPI as an estimator of the spermaceti sac length. Clicks could be attributed to the target whale because at Kaikoura sperm whales almost always surface alone and other whales are usually spaced at least one mile apart (Childerhouse et al., 1995). The target whale therefore was always the closest to the hydrophone array and produced the loudest vocalisations when the recording began. Additionally, Pamguard has two built in features which allow other whale's clicks to be filtered out: (a) a built-in click detector allows detection thresholds to be altered, rejecting all but the loudest clicks, and (b) computation of bearings to the sound sources allows signals from shallow bearings (i.e from whales further away) to be excluded. Both Options A & B are used with recordings gained via the stereo array. For recordings gained via a single hydrophone, Option B cannot be used.

3.4 Results

3.4.1 Stereo photographs and recording accessibility

A total of 172 stereo pairs were used to measure the distance between the blowhole and the posterior emargination of 21 whales. Each individual whale was encountered an average of 2.9 times (Range: 1-8) and the average number of measured photographs per whale was 8.2 (Range: 2-17). Eighty three percent of photographs were taken at a distance of < 50 metres, with the maximum distance being 67 metres. The mean number of recordings obtained per whale was 3 (Range: 1-8) and mean number of clicks analysed per whale was 645 (Range: 83-1618).

3.4.2 Errors in photogrammetric and acoustic length estimation

Repeated photogrammetric measurement of individual whales throughout a field season showed mean (and median) co-efficient of variation (CV: Standard deviation/mean) of 1.57% (Range: 0.56%-3.32%) which represents a mean error of ± 21.7 cm. Measurement in the field of the PVC calibration target demonstrated consistent camera alignment (mean CV = 0.23%). IPI measurements from individual whales recorded in the same field season had a mean CV of 0.63% (Range: 0.16%-3.13%) which represents an average error of ±0.04 milliseconds (ms).

Out of the 21 whales which were acoustically and photogrammetrically measured 12 had both sets of measurement data collected in the same encounter over more than one day (Fig 4.2). The IPI measurements were less variable compared to total length estimates derived from stereo photogrammetry.

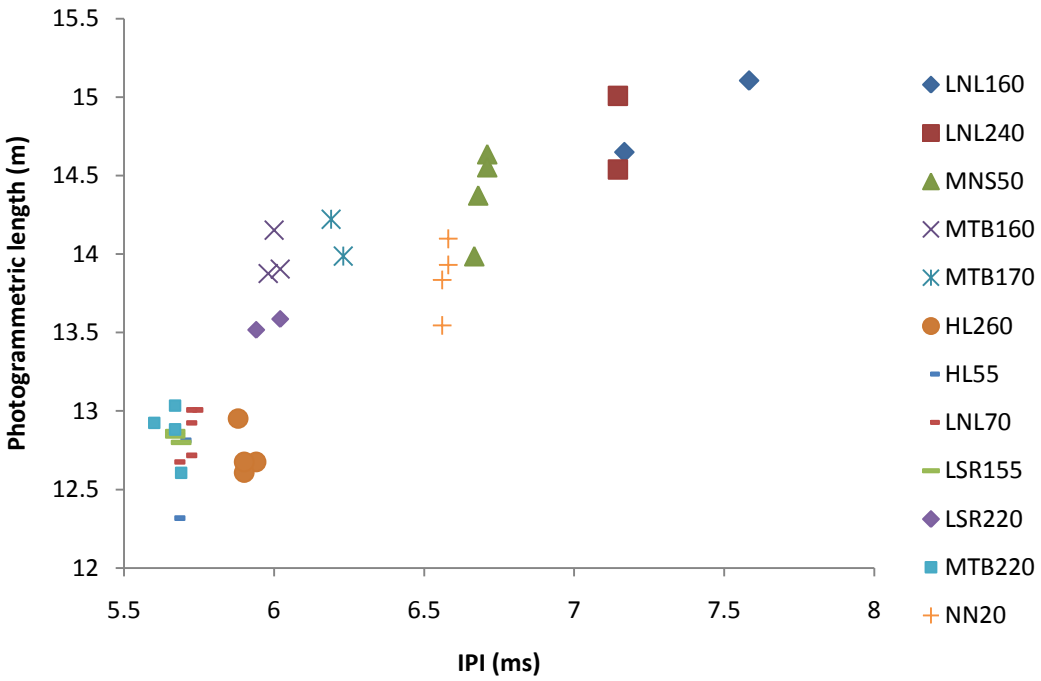

Figure 3.2 Comparison of IPI and stereo photogrammetry length estimates obtained over different encounters. Each individual whale is plotted as a different coloured shape.

3.4.3 Relationship between IPI and total length

To examine the relationship between IPI and total length the mean measurement for each was plotted for every individual whale. Linear regression of these data shows a highly significant relationship ($r^2 = 0.82$, $p < 0.001$; Fig. 3.3) giving:

$$\text{Total length (TL)} = 1.087 \cdot \text{IPI} + 6.8111 \qquad (3.2)$$

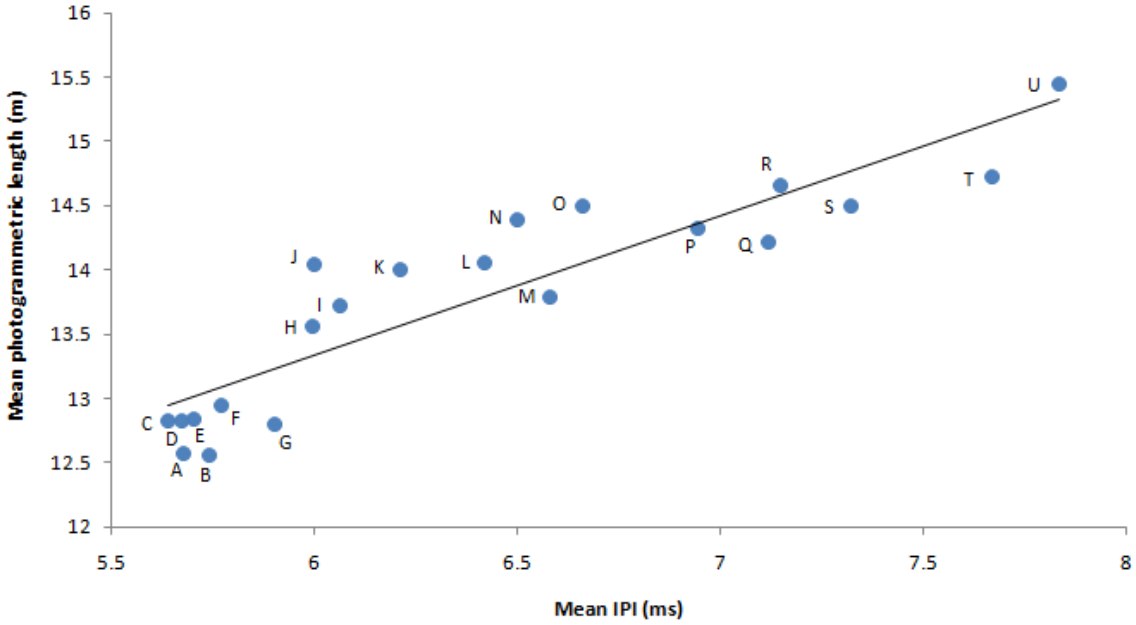

Figure 3.3 Relationship between mean IPI and mean photogrammetrically estimated total length for individual whales encountered offshore of Kaikoura. The regression line is given in the text. Individual whales are coded by letter: A (HL55), B (MTR260), C (MTB125), D (LSR155), E (LNL70), F (HR250), G (HL260), H (LSR220), I (MTB220), J (MTB160), K (MTB170), L (NN95), M (NN20), N (HR55), O (MNS50), P (MLN290), Q (HL140), R (LNL240), S (LNL160), T (MTB90) and U (MLN160).

Each recording that was used to estimate IPIs for the regression equation proposed by Rhinelander and Dawson (2004) was analysed using Miller's (2010) implementation of the Teloni (2007) cepstrum analysis method. The re-analysis of the IPIs was then compared to Rhinelander and Dawson's original photogrammetric length estimates. Following Rhinelander and Dawson (2004) a second-order polynomial was fitted and evidently provided a slightly improved fit ($r^2 = 0.79$, $p < 0.001$, Fig 3.4) compared to their analysis.

$$TL = 0.3488 \cdot IPI^2 - 3.3546 \cdot IPI + 20.586 \quad (3.3)$$

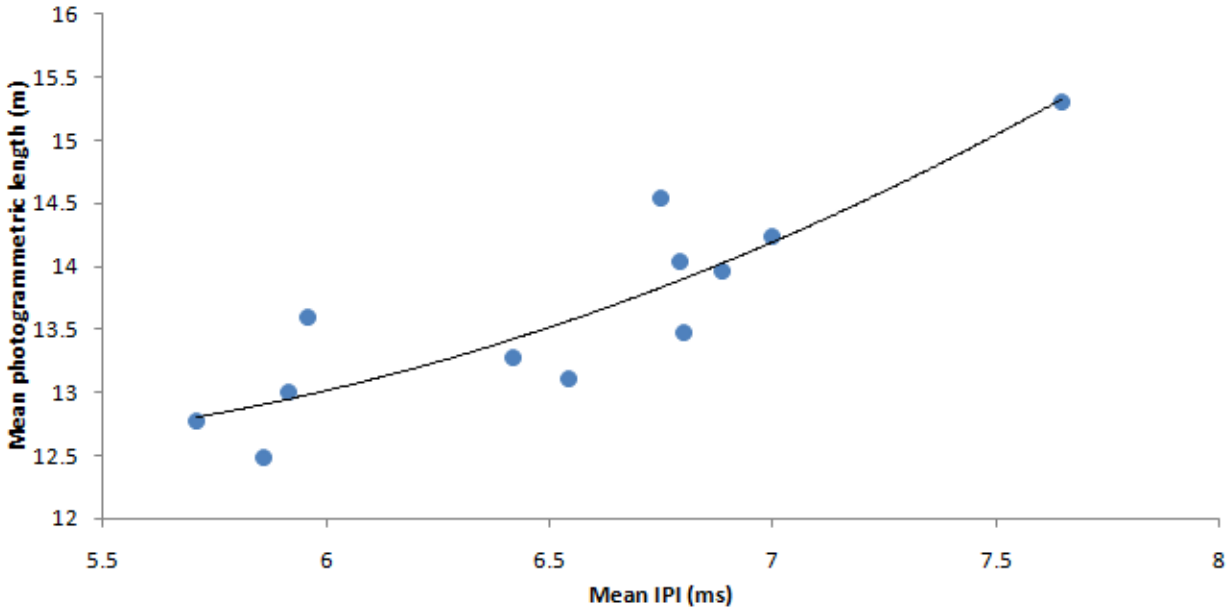

Figure 3.4 Re-computed IPIs of individual whales from Rhinelander and Dawson (2004) using the Teloni (2007) cepstrum analysis method. Mean photogrammetric lengths are unchanged. Equation is given in the text.

The re-analysed Rhinelander and Dawson (2004) IPI and photogrammetric estimates were then combined with the most recent data. This increases the sample size to 33 whales which have independently measured IPIs and total lengths. A linear regression was highly significant ($r^2 = 0.78$, $p < 0.001$, Fig 3.5), giving:

$$y = 1.1098x + 6.5724 \quad (3.4)$$

Both sets of data cover the same size range (This study; 12.56-15.45 m compared to 12.51-15.28 m, as measured via stereo photogrammetry). There was no evidence that the data sets differed significantly (t-test; p. = 0.67, d.f = 32).

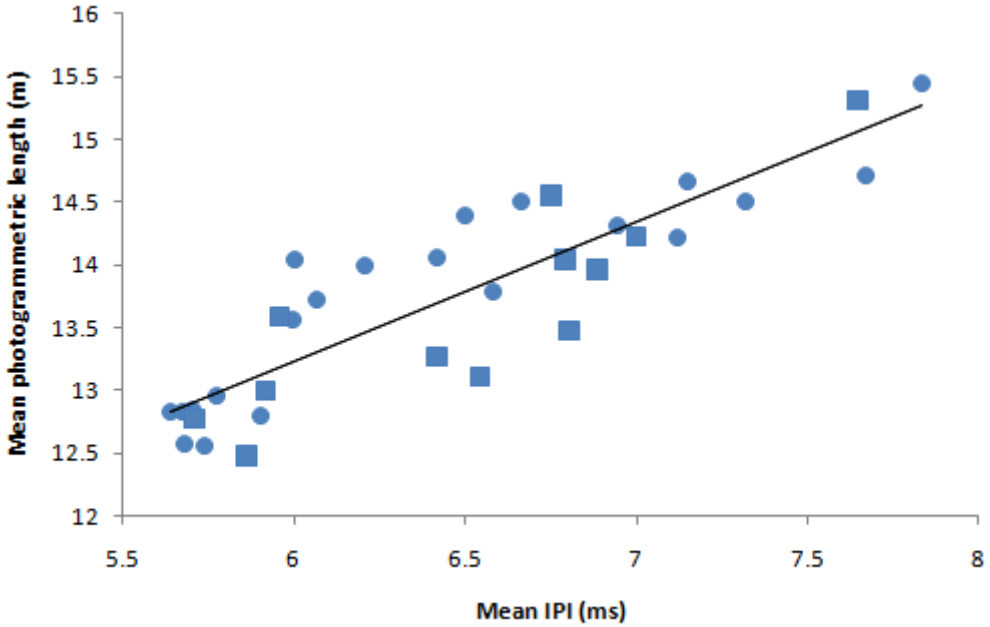

Figure 3.5 Re-analysed data from Rhinelander and Dawson (2004: squares) combined with the most recent collected data (circles). Mean photogrammetric length for each individual whale compared to corresponding mean IPI from individually identifiable whales, Kaikoura. Equation is given in the text.

3.4.4 Total length estimates using proposed equations

Differences among equations (3.2-3.4, and that of Rhinelander & Dawson 2004) estimating total length from IPI (Table 1) show that differences over the range of IPIs recorded in Kaikoura are small (Maximum difference = 62 cm).

Table 3.1 Series of IPIs covering the range recorded offshore of Kaikoura. All equations are comparing the mean photogrammetric length to mean IPI. All equations are given in the text except that published by Rhinelander and Dawson (2004).

IPI (ms)	Eq.3.2	Eq.3.3	Eq.3.4	R & D (2004) Eq.
5	12.25	12.53	12.12	12.45
5.5	12.79	12.69	12.68	12.67
6	13.33	13.02	13.23	13.02
6.5	13.88	13.52	13.79	13.50
7	14.42	14.20	14.34	14.10
7.5	14.96	15.05	14.90	14.82
8	15.15	16.07	15.45	15.67

3.5 Discussion

3.5.1 Variation in length estimates

Errors associated with measuring the distance between the blowhole and posterior emargination were small (mean C.V of multiple measurements of the same whale = 1.57%) and a substantial improvement over the previous photogrammetric techniques measuring the same body dimensions (Dawson et al., 1995, C.V = 4.35%; Gordon, 1991 C.V = 5.1%). Jaquet (2006) used a single camera and laser-rangefinder combination to measure fluke width, and reports a smaller CV (1.3%) in re-measurements of the same whale. The method developed here, however, is more accurate at estimating total length, as the distance between the blowhole and posterior emargination is a better predictor of total length than fluke width (Jaquet, 2006).

Within individuals, IPIs computed via the cepstrum method were less variable than photogrammetric length estimates (mean CV = 0.63%). This is likely to be due to two causes; 1) whales are inherently flexible, and this will affect photogrammetric accuracy (Dawson et al., 1995) and, 2) some imprecision is inevitable in locating the same points to measure each time from stereo images. IPI estimates from this study were less variable than all previous studies that have attempted to correlate this feature to an independent measure of length (Gordon, 1991, median C.V = 5.6%; Rhinelander and Dawson, 2004, mean CV 0.82%; Jaquet, 2006, median CV 1.9%). This confirms the reliability of the Teloni et al. (2007) method for measuring IPI.

3.5.2 Sperm whale length and correlation with IPI

The latest proposed regression provides the best fit between IPI and total length. Surprisingly, the best fit was found with the simplest (linear) model. Both Gordon (1991) and Rhinelander and Dawson (2004) used a 2^{nd} order polynomial models to account for Fujino's (1956) observation that the proportion of total length occupied by the spermaceti sac increases with increasing length. A 2^{nd} order polynomial was fitted to the combined data, but curved in the opposite direction to that expected, meaning that at larger IPIs total lengths decreased. Measuring body proportions of dead whales is less straightforward than it sounds because large aquatic animals distort when out of water (Klimley and Brown, 1983). It may be that Fujino's (1956) observation was not reliable.

Rhinelander and Dawson's (2004) reanalysed recordings produced IPI values that differed only slightly from the original estimates. Combining the recently collected data with the re-analysed Rhinelander and Dawson (2004) data provided the largest sample size. The fit between IPI and total length was not as good as when only the latest data was analysed. This is probably due to the use of two different stereo photogrammetric systems and the greater imprecision of the earlier system compared to the digital stereo system.

The sperm whales of Kaikoura offer some profound advantages for testing hypotheses about how the multi-pulse structure of sperm whale clicks relates to whale size, chiefly because the same individuals can be recorded repeatedly over periods from days to decades. To date, (June 2010) the longest re-sighting in this project is of NN20, which has been identified over 120 times over 18 years (Dawson, unpub. data). The main disadvantage of Kaikoura, and of other study sites beyond about 40^{o} North or South, is that females and immatures are very seldom encountered. Data reported here contain no whales' small enough to be females (Rice, 1989). Thus the relationship developed here may not be appropriate for estimating the size of small whales from their IPIs.

Of the regression equations developed from whales at Kaikoura (i.e. males) we argue that eq. 4.4 is the most reliable. While its fit is not as good as when using only the data obtained via the digital stereo photogrammetric system, it is based on the largest number of individuals.

Chapter 4: Acoustically derived growth rates of sperm whales in Kaikoura, New Zealand[4]

4.1 Abstract

We present a non-lethal method for measuring the growth of resident sperm whales based on estimating the size of animals by measuring the inter-pulse interval (IPI) of sperm whale clicks. A better model of the sound production mechanism in sperm whales has recently led to a more robust method for computing the IPI of individual animals. We have implemented this method as a software plugin for Pamguard, an open-source software package designed for passive acoustic monitoring. Using the Pamguard framework allows for both real-time IPI computation and post-processing of previously recorded whales. We demonstrate the plugin by computing the growth rates of 29 resident whales that have been recorded repeatedly off shore of Kaikoura, New Zealand between 1991 and 2009. All whales show either an increasing or stable IPI and von Bertalanffy growth curves fit the data well when whales were recorded many times over several years. Most prior knowledge of growth in sperm whales has come from fitting growth curves to size data gained from whaling or from mass strandings. The ability to track growth of individuals through time is only possible via non-lethal means, and offers a fundamentally different kind of data because differences among individuals can be measured. This type of data allows researchers to ask new and potentially more detailed questions about growth.

[4] Miller, B. Growcott, A. And Dawson, S. (in prep) Acoustically derived growth rates of sperm whales in Kaikoura, New Zealand

4.2 Introduction

Typical sperm whale vocalisations consist of broadband echolocation clicks, often showing a multiple pulse structure (Backus and Schevill, 1966). Norris and Harvey (1972) hypothesised that this multiple pulse structure arises from a single impulsive sound, created at the *museau de singe*, that is reflected within the head of the whale, and hence that time interval between these pulses represents the time taken for sound to travel the length of the spermaceti sac. Hence the hypothesis predicts that due to allometric relationships between head size and whale length, the inter-pulse interval (IPI) can be used as a measure of whale length. Gordon (1991) and Rhinelander and Dawson (2004) photographically measured whale length and quantified the relationship between photogrammetrically measured length and IPI. Gordon derived this relationship from mostly juvenile and female whales, while Rhinelander and Dawson measured pubertal and mature male sperm whales between 12.5 and 15.2 m in length.

Six of the whales in Rhinelander and Dawson's study were recorded over a span of two or more years, and five of these showed an increase in IPI. A new boat based digital stereo photogrammetric system has been developed (Chapter 2), which has resulted in the most accurate measurements of sperm whale length to date. These stereo measurements were then compared to IPI measurements of the same individuals and a new regression equation has been proposed; $y = 1.1098 \cdot IPI + 6.5724$ (Chapter 3). The acoustic data set contains several individuals that have been recorded many times, and over many years (max 19 yr), and most of the audio recordings in this data set come from photographically identified whales. A long-term data set such as this one with repeated recordings of photographically identified individuals potentially allows measurement of individual growth.

Not all sperm whale clicks show clear multi-pulse structure, therefore previous analyses applied strict criteria concerning which clicks were suitable for inclusion in the measurement of IPI (Rhinelander and Dawson, 2004). In their work, for example, analysis was restricted to clicks that had >10 dB signal-to-noise ratio, occurred between 2 - 8 min after fluke-up, and had a clear multi-pulse structure. These criteria required visual inspection of all candidate clicks.

Recent studies have shed light on the reasons for the large number of so called "unsuitable" clicks. After investigating the sound radiation pattern of sperm whale clicks Møhl et al. (2003) proposed the bent-horn model of sound production which is a refinement of the original Norris and Harvey model. In 2005 Zimmer et al. provided strong additional evidence

for the bent-horn theory which accounts for the large number of recorded clicks that do not appear to contain a clear multi-pulse structure. According to the bent horn model only on-axis clicks, recorded either directly in front of or behind the acoustic axis of the whale, exhibit the clear multi pulse structure that previous scholars refer to as IPI. The time delay between pulses of an on-axis click corresponds to the acoustic propagation delay as sound travels from the *museau de singe* reflects off the frontal sac and travels forwards out of the anterior surface of the junk. In off-axis clicks these pulses are present, but obscured by interference arising from the off-axis angle of the whale (Zimmer et al., 2005a). In the earlier studies of sperm whale IPI mentioned above, the discarded clicks were most likely to have been recorded off-axis.

It is now well established that click structure varies dramatically depending on the orientation of the whale with respect to the recording device (Mohl et al., 2003). When the multipulse structure is present, IPI can be measured and appears to be constant, but the multipulse structure is not present in every click due to off-axis distortion (Zimmer et al., 2005a). This is why Rhinelander and Dawson restricted analysis to a relatively short time window (2 - 8 min after fluke-up) in which it was assumed that the whale's orientation was likely to be reasonably constant (ie. maintaining a relatively constant angle of descent). A new approach, based on better models of sound propagation, was proposed by Teloni et al. (2007). This approach, able to extract IPIs from hundreds of clicks regardless of the presence of a clear multipulse structure, greatly facilitates a robust measure of individual size.

Adler-Fenchel (1980), Gordon (1991), Goold (1996), Rendell and Whitehead (2004), Rhinelander and Dawson (2004), have all computed inter-pulse interval from recorded sperm whale clicks using various signal processing techniques and classification criteria. One thing common to all of the above listed methods is that they attempt to compute the IPI from a small number of selected individual clicks. Adler-Fenchel used a ranking system to score whether or not clicks were selected for analysis, and IPI measurements were made by manually measuring the distance between peaks in the time domain. Gordon also measured the IPI from the time domain waveform, but only used "usual" clicks recorded 2-8 minutes after the whale fluked and discarded all others. These clicks were found to be more likely to contain a clearly defined multi-pulse structure than clicks recorded later in the dive. Goold (1996) applied the signal processing techniques of cepstral analysis as well as autocorrelation analysis to compute the IPI. Rendell and Whitehead (2004) applied cepstral analysis to compute the IPI of coda clicks from whales that were presumably near the ocean

surface, while Rhinelander and Dawson used autocorrelation analysis and, like Gordon (1991), only analysed clicks that were recorded 2 - 8 minutes after the whale dived. In all of these studies large numbers of recorded clicks were considered unsuitable for analysis and ultimately discarded.

Teloni et al. (2007) proposed that despite off-axis clicks being dominated by off-axis pulses, they still retain pulses that correspond to the twice the distance between the *museau de singe* and the frontal sac. They postulated that the ensemble average of the cepstrum of hundreds of clicks should yield a consistent estimate of IPI. Cepstral techniques have long been used to identify reflections of broadband signals (Bogert et al., 1963) and ensemble averaging is a long-standing technique in signal processing. Even before the bent-horn model, ensemble averaging was employed to obtain stable estimates of sperm whale IPI. In a study of the potential for acoustic identification of sperm whales Dougherty (1999) suggested using the ensemble average of autocorrelation functions for 75 sequential clicks to obtain a stable estimate of the IPI. The method of Teloni et al. (2007) is not only objective, which facilitates automation, but also more relaxed than previous criteria for computing IPI, and hence allows for analysis of additional recordings not previously considered suitable for IPI measurement, increasing sample size.

4.3 Methods

Data for this project were collected from 1990 - 2009 as part of a long-term research program off Kaikoura, New Zealand conducted by Otago University's Marine Mammal Research Group. In brief, data collection involved making acoustic recordings of photographically identified (Arnbom, 1987; Childerhouse et al., 1996) whales. Field work from 1990-2000 was previously described by Rhinelander and Dawson (2004). All recordings analysed in the original study by Rhinelander and Dawson (2004) were made directly behind whales after they fluked up to ensure that the first 8 minutes of recordings contained primarily on-axis clicks as the whale descended, however the ensemble average technique implemented in the Pamguard plugin permits analysis of additional recordings from outside that 8 minute time period as well as recordings made from aspects other than directly behind the whale.

Archived recordings made with the Uhër 4400 report monitor analog tape recorder (1990 to 1995) had to be restored before digitisation could occur. This is because the adhesive which binds the oxide to the tape film is capable of absorbing water from the atmosphere if humidity levels are too high; this results in the breakdown of the adhesive (Ciletti, 2006). Playing the tapes in this condition will damage them and result in poor fidelity due to a build up of oxide

on the tape heads. To re-activate the adhesive the affected tapes were baked in an oven at 55 degrees celsius for eight hours (Nigel Bunn, pers. comm.) before digitisation could occur.

Additional photographic and acoustic data collection occurred in 2002 and from 2005 - 2009. In 2002 recordings were made with the same Sonatech 8178 hydrophone, Sony TCDD10-PROII Digital Audio Tape recorder, and protocols for acoustic recording and photographic identification from 1996 - 2000. Recordings from 2005 to present were made with a custom-built stereo hydrophone array (Barlow et al., 2008) and a laptop running Ishmael software with a National Instruments DAQ6062E data acquisition card (2005-2006) or an Edirol R4 hard disk recorder (2007-2009). Hydrophones in the stereo hydrophone array were not individually calibrated, but an identical array had a reasonably flat (±4 dB) frequency response from 1 to at least 40 kHz (Barlow et al., 2008). The Edirol R4 and National Instruments 6062E were set to 96 kHz sample rate and had a flat frequency response from 10 Hz - 40 kHz (-3 dB). The requested sample rate and the actual sample rate of the 6062E were not the same, so the actual sample rate of the 6062E was determined using a pinger that made a tone at a known frequency of 10.100 kHz. After applying this correction it was determined that the 6062E actually recorded at a sample rate of 99.948 kHz. The 6062E data acquisition card sampled with 12-bit precision, while the Edirol R4 was set to either 24 or 16-bit precision. Pamguard (version 1.6) was only capable of using 16-bit wav files, so 12 and 24-bit recordings were converted to 16-bit wav files before analysis. The hydrophone elements on the stereo array were spaced 5 m apart and the deepest element was deployed to a depth of either 65 or 105 m.

A custom software plugin implementing the IPI computation method from Teloni et al. (2007) was developed for the computer program Pamguard. Pamguard is freely available, open source software for passive acoustic monitoring (Gillespie et al., 2008). The open nature of this software encourages collaboration between researchers. Pamguard has a modular architecture that facilitates the development of plugins for exploring new research techniques. The IPI plugin presented here depends on a substantial amount of basic functionality provided by Pamguard core modules. Existing Pamguard plugins used in this study include the hydrophone array manager, multi-channel data acquisition (both from live input and archived audio files), bandpass filters, and click detection (Fig 4.1).

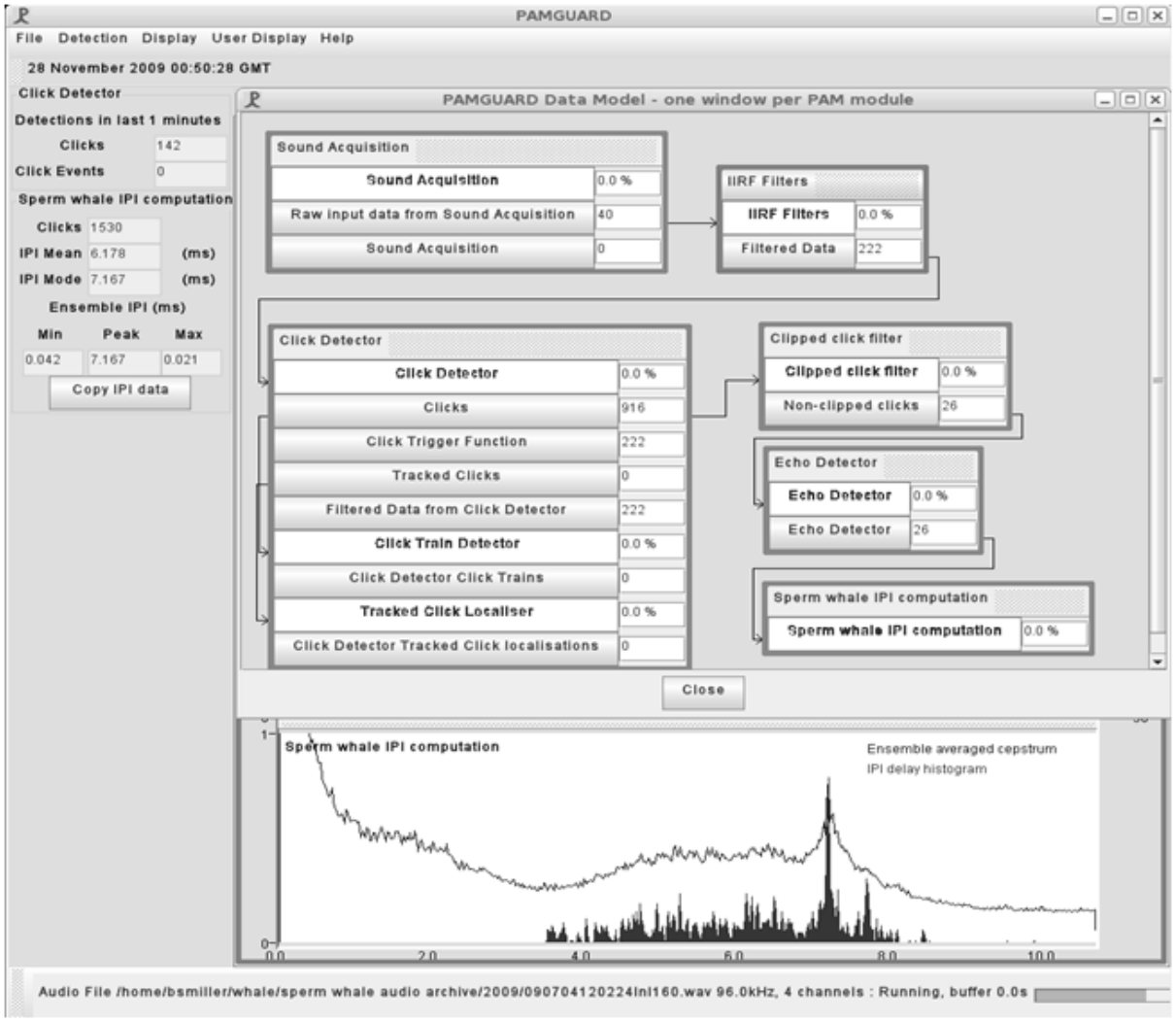

Figure 4.1 Screen shot of Pamguard IPI plugin showing output and data flow.

Acoustic data were first high-pass filtered with an 8th order Butterworth filter using Pamguard's IIR filter module with the corner frequency set to 1.5 kHz. Filtered data were then input into Pamguard's built-in click detector. For single hydrophone recordings, the click detection threshold was set so that detected clicks correspond to those from the target whale (which was typically the loudest in a recording). For stereo recordings the click detection threshold was usually set lower, and the built-in angle vetoes of the click detector were adjusted so that only clicks coming from the target whale were kept. The angle veto works by excluding clicks from further analysis if they have a bearing that is dramatically different than that of the target whale. The length window for detected clicks was set to 40 ms with 10 ms pre-sample and 30 ms post-sample. Detected clicks were then used as input into the IPI computation plugin.

IPI measurement followed the methods outlined by Teloni et al. (2007) and to a lesser extent Rhinelander and Dawson (2004). Before IPI measurement, the IPI plugin filtered any clicks that had more than three consecutive samples within 90% of the full scale amplitude to exclude clicks that had been clipped. Next, the cepstrum of each individual click was computed as

$$Ct = |FFT^{-1}(\log|FFT(x_t)|) \quad (4.1)$$

Where x_t is the digital representation of the time domain waveform and FFT and FFT^{-1} are the fast Fourier transform and inverse fast Fourier transform respectively as in Teloni et al. (2007). The time delay at the peak of the cepstrum was stored as the IPI of that click and used to create a histogram of IPI for each recording. On a basic level this IPI histogram was similar to the methods used by Rhinelander and Dawson (2004), who estimated the IPI from the autocorrelation function of individual clicks and then computed the mean and standard error of all IPIs. In addition to constructing the IPI histogram, the plugin also computes the ensemble average of the cepstrum from all detected clicks. The peak value of the ensemble average of the cepstrum was located and the time delay of the peak kept as the *ensemble IPI* as described by Teloni et al. (2007). The *ensemble IPI* computation allows analysis of recordings that were made from arbitrary locations with respect to the whale. Implementing both methods in the module requires little extra processing and facilitated comparison of the methods (see section below).

The peak width of the *ensemble IPI* was used as the measure of uncertainty for each recording. Peak widths were measured at 75% of the maximum value. A threshold width of 1 ms was used to exclude measurements with high uncertainty (typical IPI values range from 3 - 9 ms). Out of 279 analysed recordings, only two were excluded due to high uncertainty. To validate the ensemble average technique we compared the IPI histogram and ensemble IPI results from the Pamguard IPI plugin to the IPIs of 36 recordings from the same data set that had been analysed previously by Rhinelander (2001).

For the computation of acoustic growth rates all recordings of each individual whale were considered for analysis if the total time between first and last recordings spanned six months or more. IPIs from these recordings were obtained using the Pamguard IPI plugin, and a von Bertalanffy growth curve (von Bertalanffy, 1938) fitted to the IPIs. The von Bertalanffy growth curve has been used to measure growth of female sperm whale populations

(Evans and Hindell, 2004) and takes the form of:

$$L(t) = L_{\infty} (1\text{-}ce^{-kt}) \qquad (4.2)$$

where L(t) is the IPI (in milliseconds) at time t, L_{∞} is the asymptotic (maximum) IPI possible, c is a constant of integration, the positive number k is the growth rate, and the time t is measured in years. Growth curves were fitted in Matlab using the nonlinear least squares fitting algorithm. To avoid unrealistically large asymptotic IPIs and growth rates, values for L_{∞} and k were restricted to be between 1 - 9.5 ms and 0 - 1 respectively.

4.4 Results

4.4.1 Comparison of IPI computation methods

There was good correspondence among the different methods over all 36 recordings. For these recordings the number of detected clicks used by the Pamguard plugin for IPI measurement ranged from 105 - 2604, while the number of clicks used by Rhinelander and Dawson ranged from 6 - 45. Linear regression between IPI estimates made with the Pamguard IPI plugin and those computed by Rhinelander and Dawson (2004) reveal an excellent one-to-one relationship (Fig 4.2). The goodness of fit for the ensemble IPI - Rhinelander IPI had an r^2 value of 0.95, while the modal value from the IPI histogram had $r^2 = 0.36$ showing that the ensemble IPI method provides the most similar results to those used by Rhinelander and Dawson (2004). An interesting result is that these automated methods work surprisingly well even with as few as 105 clicks. Teloni et al. (2007) suggested using at least 1000 clicks for stable results, however the present results indicate that fewer clicks can be used under some circumstances e.g. when using high quality recordings made directly behind the whale after fluke up.

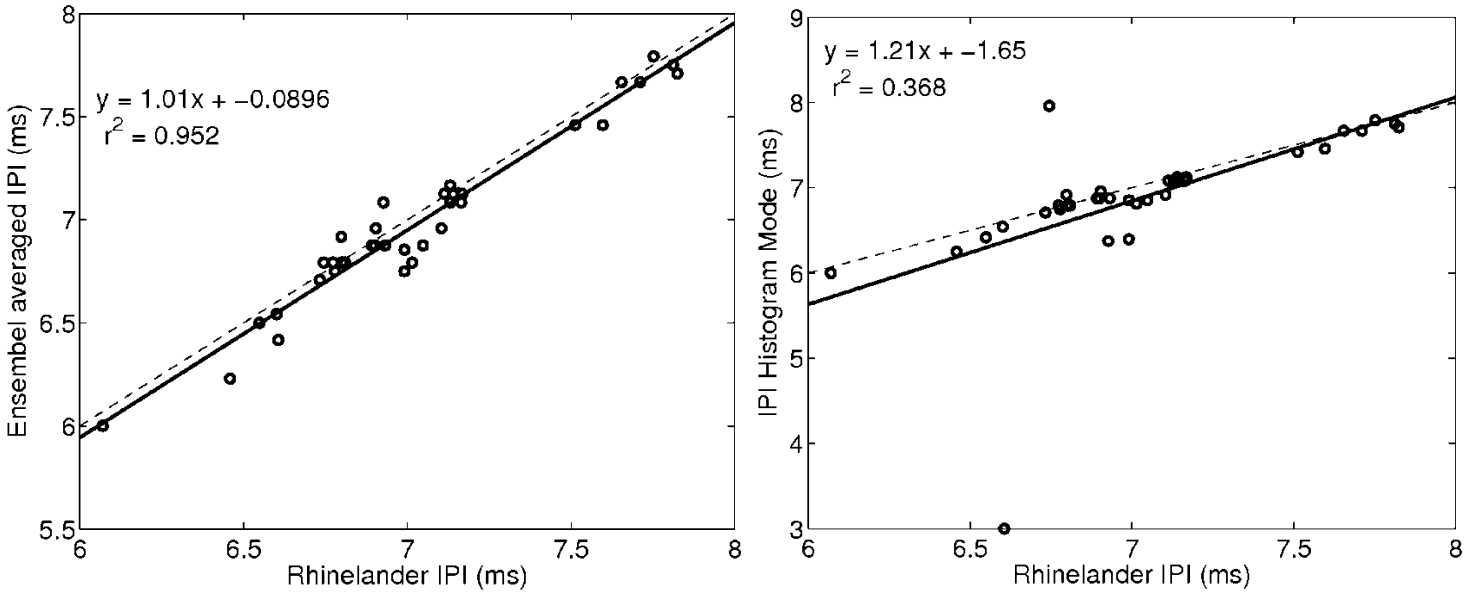

(A) **(B)**

Figure 4.2 Comparison of interpulse intervals (IPIs) computed by Rhinelander and Dawson (2004) with (A) Pamguard IPI plugin ensemble average and (B) IPI histogram mode. Dotted line shows a perfect one-to-one relationship.

4.4.2 Acoustic growth rates in Kaikoura

Thirty-two whales were recorded over multiple field seasons, and all whales showed either an increasing or stable IPI over time (Fig 4.3). Von Bertalanffy growth curves were fit to IPIs of 29 whales. Three of the whales had only two recordings, thus a von Bertalanffy curve could not be fitted, however two of these whales (HR25 and NN40) showed an increase in IPI over time. Von Bertalanffy growth curves were an excellent fit for 24 whales that showed increase in IPI over time, but were a poor fit for the five whales that had relatively stable IPIs (Table 4.1). Excluding these five whales, the mean r^2 for the remaining fits was 0.93 (0.75 - 0.99 range). Asymptotic maximum IPIs, L_∞, ranged between 5.9 - 9.5 ms and the growth rate constant ranged from 0.01 - 1.

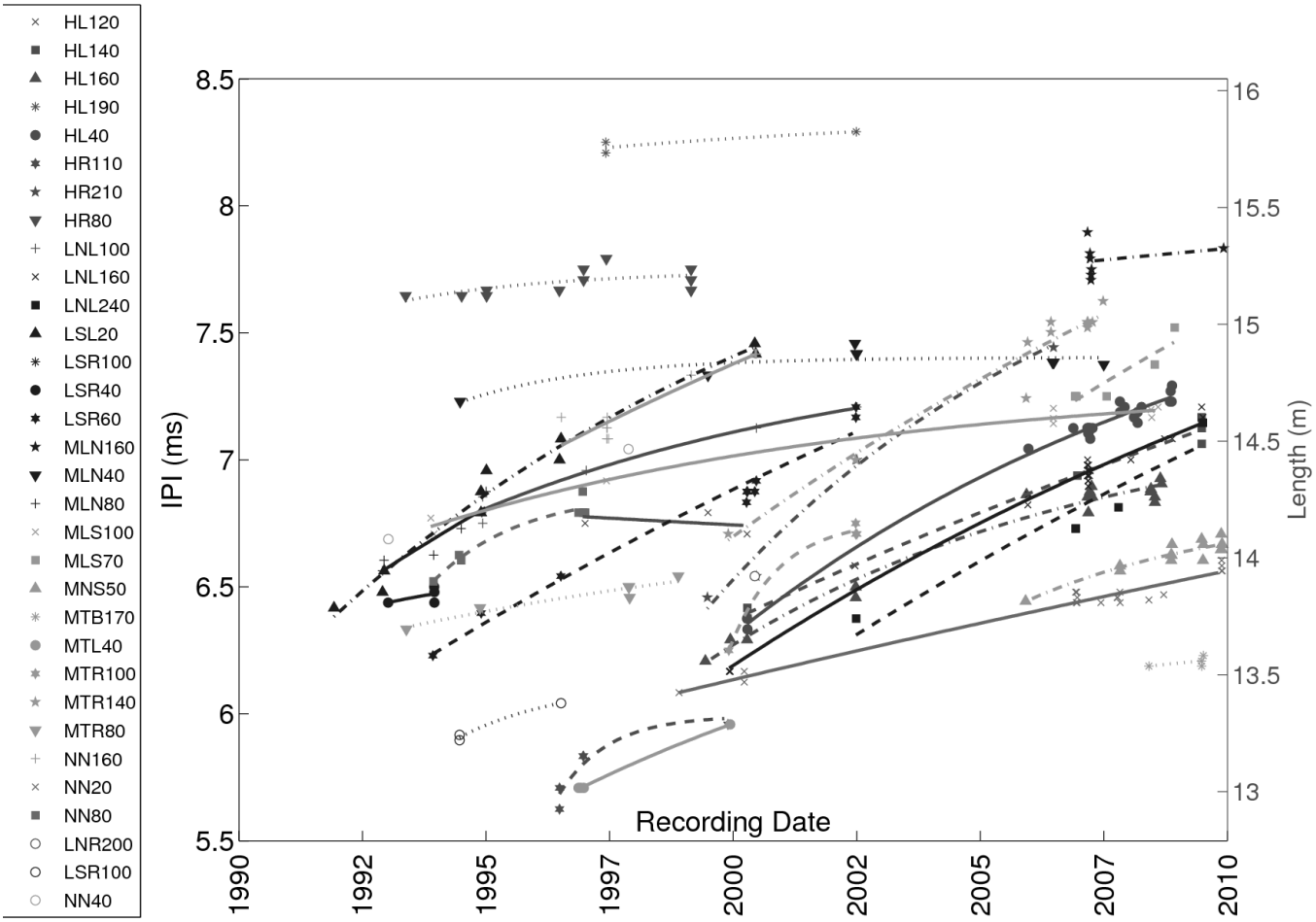

Figure 4.3 Interpulse interval (IPI) measurements of 32 different whales from 1991-2008. Points show ensemble average IPIs from independent recordings. Lines are the fitted von Bertalanffy growth curves from Table 4.1. Lengths are derived from the regression equation y = 1.1098x + 6.5724 (Chapter 3).

Table 4.1 Fitted von Bertalanffy growth rate parameters for 29 whales. See text for parameter description.

Whale	N	Years	L_∞	k	c	SSE	r^2
HL120	4	3.33	6.122	0.016765	-0.10685	0.00383183	0.2072
HL140	6	9.2	9.222	0.032066	0.30648	0.00639951	0.99
HL160	21	9.24	7.207	0.12942	0.13959	0.0295774	0.978
HL190	3	5.07	8.371	0.11589	0.016935	0.000881892	0.75
HL40	25	8.6	7.968	0.093799	0.20253	0.0159305	0.9877
HR110	5	3.41	5.992	1	0.051342	0.00653756	0.9009
HR210	5	7.01	8.17	0.12763	0.21478	0.00981822	0.9846
HR80	11	5.78	7.746	0.3146	0.015332	0.0152298	0.3992
LNL100	6	7.58	7.475	0.11962	0.089928	0.00549206	0.9657
LNL160	28	9.59	8.621	0.052462	0.28313	0.0276559	0.9861
LNL240	6	7.02	9.5	0.03808	0.33574	0.0383106	0.9083
LSL20	11	8.54	8.335	0.092057	0.23421	0.0236916	0.9836
LSR100	3	2.05	6.123	0.47882	0.035349	0.000220272	0.9823
LSR40	4	0.935	6.567	0.33114	0.0196	0.00199415	0.3058
LSR60	10	8.56	9.5	0.036396	0.34363	0.0261276	0.9703
MLN160	8	2.75	8.302	0.036725	0.062768	0.0237295	0.1322
MLN40	8	13	7.404	0.38054	0.023884	0.00826444	0.7544
MLN80	6	2.1	9.483	0.042632	0.30793	0.0101262	0.8614
MLS100	9	14.7	7.315	0.10702	0.079037	0.00509956	0.9839
MLS70	6	2.02	9.5	0.053367	0.23864	0.00951328	0.8476
MNS50	15	3.98	6.818	0.23061	0.055042	0.00873991	0.8499
MTB170	4	1.1	6.298	0.19205	0.017536	0.000817752	0.2816
MTL40	4	3.07	6.695	0.096516	0.14806	4.92656e-05	0.9989

MTR100	4	2.59	6.763	0.98479	0.075787	0.00120497	0.9928
MTR140	11	7.59	9.5	0.049943	0.29638	0.0433166	0.947
MTR80	6	5.5	6.812	0.088219	0.06921	0.00225263	0.919
NN160	13	3.95	9.5	0.040418	0.25716	0.0240711	0.8999
NN20	20	11	9.28	0.014633	0.34446	0.0139188	0.9637
NN80	8	3.07	6.876	0.55481	0.051355	0.00576211	0.946

4.5 Discussion

In general von Bertalanffy growth curves were a good model for describing change in IPI of sperm whales as a function of time. Of the five whales for which the von Bertalanffy model was a poor fit, two (whales LSR40, and MTB170), were only recorded over a year or less, while the other three whales, (MLN160 HL120, HR80) showed a stable IPI over the three and six years which they were recorded (Fig 4.3).

Because IPI is correlated with whale size (Gordon, 1991; Rhinelander and Dawson, 2004) we can conclude that most of the whales observed repeatedly in Kaikoura are still growing. Most literature on growth of male sperm whales comes from age-length records of whale catches (Nishiwaki et al., 1963; Rice, 1989). Applying the equation suggested in Chapter 3 or Rhinelander and Dawson (2004) to these IPI estimates allows us to estimate whale length (second vertical axis in Fig 4.3). When combined with photographic identification, the acoustic methods presented here allow for non-lethal measurements of the growth of individual whales.

While growth of individuals could be measured using photogrammetric techniques only (eg. Webster et al. 2009), there are several advantages to the acoustic methods presented here. Stereo photography requires manoeuvring alongside of the whale (Dawson et al., 1995), which can cause the whale to turn away or dive early, especially when other vessels (such as whale watching boats) are present (Richter et al., 2006). Additionally, identification photographs of the whale must be taken from directly behind the whale, thus requiring additional manoeuvring. In contrast, audio recordings of the whale can be made from any position, including behind the whale, which facilitates rather than conflicts with the photographic identification efforts. Stereo photogrammetry presently requires a somewhat

cumbersome system of two cameras on either end of a 2.4 m bar, attached, at eye height, to a short mast. Analysis of the image requires expensive proprietary software. IPI measurements can be made using a single hydrophone, field recorder, and free open source software. Laser photogrammetric systems offer simpler logistics and analysis and have been used successfully on other cetaceans (Durban and Parsons, 2006; Rowe and Dawson, 2008; Webster et al., 2009), however our own attempts using laser systems on sperm whales offshore of Kaikoura were unsuccessful. Laser dots from relatively powerful (Aimshot LS8200; 12mW) green lasers, intended for use with firearms, were not visible on whales 50m away (the present limit of approach in Kaikoura).

There are some inherent limitations when measuring growth rates of sperm whales acoustically. Unless the researcher is able to track individual whales at depth using a 3 dimensional hydrophone array, the approach cannot be used when multiple whales are diving in close proximity. Hence it is more practical at higher latitudes, where whales are typically spaced further apart (Gaskin, 1970). In nursery groups where many whales are closely grouped together and dive in synchrony, it is unlikely that IPIs could successfully be matched to particular individuals.

It should be noted that the limitation stated above arises from the inability to match photographs with acoustic records for nearby individuals and not from any inherent limitation in the Pamguard IPI plugin. In fact a yet unexplored use of this plugin would be to estimate the size structure in groups of whales encountered during acoustic surveys (eg. Barlow and Taylor, 2005). Acoustic bearings and angle vetoes (both core Pamguard modules) could be used to separate clicks from different whales and each bearing trace could be used as input into a separate instance of the IPI plugin. This could yield valuable information on population structure with a minimum of additional survey effort.

Chapter 5: Conclusion

The three main objectives of this thesis were to;

1) To develop a new boat based digital stereo photogrammetry system and assess its measurement accuracy (Chapter 2).

2) Improve the relationship between IPI and total length via increasing the sample size of measured whales, and via applying improved photogrammetric and acoustic analysis methods (Chapter 3).

3) Acoustically estimate growth rates of seasonal resident sperm whales that have been recorded multiple times at Kaikoura (Chapter 4).

5.1 Development of a digital stereo photogrammetry system to measure cetaceans at sea

The development of the new boat-based stereo photogrammetric system and subsequent test of measurement accuracy has shown that it is ideally suited for measuring sperm whale length. Mean measurement error was 0.82% over the entire distance/angle network tested.

This new system design and implementation is a substantial improvement on the analog system used by Dawson et al. (1995). The system is easier to use at sea and its images are easier and quicker to measure because stereo measurements are now made using *Australis* software rather than an expensive and difficult-to-use analog stereo plotter. *Australis* also has a in-built self calibration feature, which makes estimating the interior and exterior orientation parameters relatively easy. Crucially, repeated measurements of the same whale are about three times more precise with the new method compared to Dawson et al. (1995).

The application of this new digital system to other research projects is more attractive. The new system requires no specialised equipment and *Australis* is flexible in that it can accommodate a variety of off-the-shelf cameras. The system is already suitable for measuring large whales, but it would be relatively easy, for example, to adapt this system to measure dolphins at close range. Finally, the system is relatively cheap to develop. Without taking into account the cost of *Australis*, which was available to use through the University of Otago Surveying department, the hardware cost of the system was approximately $1500 NZ.

5.2 Measuring whales from their clicks: a new relationship

A new empirical relationship between IPI and total length has been developed using newly developed photogrammetry and IPI estimation methodologies. The Pamguard plugin developed by Miller (2010) averages the cepstrum of a series of clicks (Teloni et al., 2007) and allowed automated IPI computation. This approach has the inherent advantages of greater objectivity and repeatability and facilitates analysis of a much larger sample size.

Using these two new methods, I was able to estimate IPIs and total lengths of 21 individually identified sperm whales. This is substantially more than had been measured previously (12, Rhinelander and Dawson, 2004; 11, Gordon, 1991). These new measurements combined with reanalysed data from Rhinelander and Dawson (2004) have allowed a new equation to be proposed based on 33 whales. This equation has a better fit than any other published for this purpose. Improved fit probably results from improved accuracy and precision of both the new digital stereo camera system and the newly developed IPI estimation method (Teloni et al., 2007). When investigating the size structure of other high latitude populations this new equation should be preferred.

5.3 Acoustically derived growth rates of sperm whales in Kaikoura, New Zealand

Sperm whales located offshore of Kaikoura are unique in that they are easily accessible and have been subject of study since 1990. These factors combined with the fact that some individuals are resident at Kaikoura for long periods, and/or return regularly allows questions such as individual growth to be investigated.

Previous work that analysed IPIs was strongly limited by the time it took to analyse recordings (eg. Rhinelander, 2002). This was because each single click had to be visually assessed and measured by hand. With the development of an automated IPI methodology, archived recordings of individuals, spanning multiple field seasons, were able to be analysed. Most sperm whales were found to have an increasing IPI which represents growth. Von Bertalanffy growth curves fitted most individuals well – those showing poor fits generally had the least data, so a lack of fit was not surprising.

This is the first time that growth rates have been estimated acoustically. Because this process is non-invasive, individuals can be tracked through time. Also, because the process can be applied to any good quality recording of sperm whales, it opens up a much larger dataset for

analysis. Even in the case of individual identities being unknown, this approach allows robust data on population size structure to be gathered from archived or new recordings.

5.4 Future research possibilities

The research described in this thesis sets the scene for projects that might follow. Such future research could include:

- Measurement of features on sperm whale flukes, in order to document the size of nicks, scallops and spacing between tooth rakings and hence gain insight into predation on sperm whales. In addition, fluke width could also be compared to total length and/or IPI of the same individual. Equations could then be derived, similar to Jaquet's (2006) study, except total length would be estimated from the same individual instead of from whaling data. This improvement could possibly lead to a closer fit between fluke width and total length.

- Does the size distribution of the population change between seasons, and has it changed over the two decades of study so far?

  Theory predicts that during the breeding season the large individuals should leave to join nursery groups of females and calves in the tropics. Are whales that leave Kaikoura at this time especially large?

- Individuals at Kaikoura appear to show small scale habitat preferences. Is this influenced by the size of the individual?

References

Alder-Fenchel, H. S. (1980) Acoustically derived estimates of the size distribution for a sample of sperm whales ~*Physeter catodon*, in the Western North Atlantic. *Canadian Journal of Fish and Aquatic Science*. **37**: 2358–61.

Amudin, M. (1978) Sperm whale clicks: Pulse Interval in Clicks from a 21 metre specimen. Ph.D. thesis. Stockholm University.

Angliss, R. Rugh, D. Withrow, D. and Hobbs, R. (1995) Evaluations of Aerial Photogrammetric Length estimates of the Bering-Chukchi-Beaufort Seas Stock of Bowhead whales (*Balaena mysticetus*). *Report of the International Whaling Commission.* **45**: 313-324.

Arnbom, T. (1987) Individual identification of sperm whales. *Report of the international Whaling Commission*. **37**: 201-204.

Backus, R. H. and Schevill, W. E. (1966) "Physeter clicks", *in Whales, Dolphins, and Porpoises*. University of California Press. 510-528.

Barlow, J. Rankin, S. and Dawson, S. (2008). A guide to constructing hydrophones and hydrophone arrays for monitoring marine mammal vocalizations. *Technical Report 417, NOAA Technical Memorandum NMFS*.

Barlow, J. and Taylor, B. (2005) Estimates of sperm whale abundance in the Northeastern temperate Pacific from a combined acoustic and visual survey. *Marine Mammal Science.* **21(3)**: 429–445.

Best, P. B. (1979) Social organisation of sperm whales, *Physeter macrocephalus*. In *Behaviour of marine mammals* Vol. 3: *Cetaceans.* (eds. Winn, H.E. and Olla, B.C.) Plenum Press, New York. 510-528.

Best, P. B. (1990) A note on proportional body measurements in sperm whales. *Report of the International Whaling Commission*. SC/42/sp9 (unpublished).

Best, P. B. and Ruther, H. (1992) Aerial photogrammetry of southern right whales, *Eubalaena australis. Journal of Zoology (London)*. **228**: 595-614.

Bogert, B. P. Healy, M. J. R. and Tukey, J. W. (1963) The quefrency analysis time series for echoes: cepstrum, pseudoautocovariance,cross-cepstrum, and saphe cracking.(eds. Rosenblatt, M.) In: *Symposium on Time Series Analysis*. Wiley, New York. 209-43.

Brager, S. and Chong, A. (1999) An application of close range photogrammetry in dolphin studies. *Photogrammetric Record*. **16(93)**: 503-517.

Calambokidis, J. Steiger, G. H. Cubbage, J. C. Balcomb, K. C. and Prentice, B. (1989) Biology of humpback whales in the Gulf of the Farallones. Final report to Gulf of Farallones National Marine Sanctuary. San Francisco.

Ciletti, E. (2006) If I Knew You Were Coming I'd Have Baked A Tape: A Recipe for Tape Restoration. Accessed 4th June 2010. http://www.tangible-technology.com/tape/baking1.html.

Childerhouse, S. J. Dawson, S. and Slooten, E. (1995) Abundance and seasonal residence of sperm whales at Kaikoura, New Zealand. *Canadian Journal of Zoology* **73**: 723-31.

Childerhouse, S. J. Dawson, S. and Slooten, E. (1996) Stability of fluke marks used in individual photo identification of male sperm whales at Kaikoura, New Zealand. *Marine Mammal Science*. **12(3)**: 447–451.

Chong, A. K. and Schneider, K. (2001) Two-Medium Photogrammetry for Bottlenose Dolphin Studies. *Photogrammetric Engineering & Remote Sensing*. **67(5)**: 621–628.

Christal, J. and Whitehead, H. (1997) Aggregations of mature male sperm whales on the Galapagos island breeding ground. *Marine Mammal Science*. **13**: 59-69.

Clark, M. R. (1978) Structure and proportion of the spermaceti organ in the sperm whale. *Journal of the Marine Biological association of the United Kingdom.* **58**: 1-17.

Clarke, M. R. (1979) The head of the sperm whale. *Scientific American*. **240(1)**: 106-117.

Cooke, J. G. De La Mare, W. K. and Beddington, J. R. (1983) Some aspects of the reliability of the length data for the Western North Pacific stock of sperm whales. *Report of the International Whaling Commission*. **33**: 265-268.

Cranford, T. Amundin, M. and Norris K. (1996) Functional Morphology and Homology in the Odontocete Nasal Complex: Implications for Sound Generation. *Journal of Morphology*. **228**: 223-285.

Cranford, T. (1999) The Sperm whale's nose: Sexual selection on a grand scale? *Marine Mammal Science*. **15(4)**: 1133-1157.

Cubbage, J.C. and Calambokidis, J. (1987) Size-class segregation of Bowhead whales discerned through aerial stereophotgrammetry. *Marine Mammal Science.* **3**: 179-85.

Dawson, S. M. Chessum, C. J. Hunt, P. J. and Slooten, E. (1995) An inexpensive, stereophotographic technique to measure sperm whales from small boats. *Report of the international Whaling Commission*. **45**: 431–436.

Dougherty, A. M. (1999) Acoustic identification of individual sperm whales (*Physeter macrocephalus*). Master's thesis, University of Washington.

Durban, J. W. and Parsons, K. M. (2006). Laser-metrics of free ranging killer whales. *Marine Mammal Science*. **22**: 735–743.

Drouot, V. Gannier, A. and Goold, J. (2004) Diving and feeding behaviour of sperm whales (*Physeter macrocephalus*) in the northwestern Mediterranean Sea. *Journal of Aquatic Mammals.* **30**: 419-26.

Dunn, J. L. (1969) Airborne measurements of the acoustic characteristics
of a sperm whale. *Journal of the Acoustic Society of America*. **46**: 1052–1054.

Durban, J. W. and Parsons, K. M. (2006) Laser-metrics of free ranging killer whales. *Marine Mammal Science*. **22:** 735–743.

Evans, K. and Hindell, M. (2004) The age structure and growth of female sperm whales (*Physeter macrocephalus*) in southern Australian waters. *Journal of Zoology*. **263(3)**: 237–250.

Flewellen, C.G. and Morris, R.J. (1978) Sound velocity measurements on samples from the spermaceti organ of the sperm whale (*Physeter catodon*). *Deep-Sea Research*. **25**: 269-77.

Fujino, K. (1956) On the body proportions of the sperm whale (*Physter catodon*). *Scientific Report of the Whales Research Institute Tokyo*. **11**: 47-83.

Gaskin, D. E. and Cawthorn, M. W. (1967) Diet and feeding habits of the sperm whale (*Physeter Catodon L*.) in the Cook Strait region of New Zealand. *New Zealand Journal of Marine and Freshwater Research*. **1(2)**: 156-179

Gaskin, D. E. (1970) Composition of schools of sperm whales *Physeter catodon linn*. east of New Zealand. *New Zealand Journal of Marine and Freshwater Research*. **4(4)**: 456-71.

Gillespie, D. Gordon, J. Mchugh, R. Mclaren, D. Mellinger, D. Redmond, P. Thode, A. Trinder, P. and Deng, X. (2008) Pamguard: Semiautomated, open source software for real-time acoustic detection and localisation of cetaceans. *Proceedings of the Institute of Acoustics*, 30: Pt 5.

Goold, J. C. D. (1996) Signal processing techniques for acoustic measurement of sperm whale body lengths. *The Journal of the Acoustical Society of America*. **100**: 3431-41.

Goold, J. C. and Jones, S. E. (1995) Time and frequency domain characteristics of sperm whale clicks. *The Journal of the Acoustical Society of America*. **98**: 1279-91.

Gordon, J. C. D. (1987) The behaviour and ecology of Sperm whales off Sri Lanka. Ph.D. thesis. University of Cambridge.

Gordon, J. C. D. (1990) A simple photographic technique for measuring the length of whales from boats at sea. *Report of the international Whaling Commission*. **40**: 581-88.

Gordon, J. C. D. (1991) Evaluation of a method for determining the length of sperm whales (*Physeter catodon*) from their vocalizations. *Journal of Zoology, London*. **224**: 301-14.

Jaquet, N. (2006) A simple photogrammetric technique to measure sperm whale at sea. *Marine Mammal Science*. **22**: 862-79.

Jaquet, N. and Whitehead, H. (1996) Scale-dependant correlation of sperm whale distribution with environmental features and productivity in the South Pacific. *Marine Ecology Progress Series*. 135: 1-9.

Jaquet, N. Dawson, S. Slooten, E. (2000) Seasonal distribution and diving behaviour of male sperm whales off Kaikoura: foraging implications. *Canadian Journal of Zoology.* **78**: 407-19.

Jaquet, N. Dawson, S. and Douglas, L. (2001) Vocal behaviour of sperm whales: Why do they click? *The Journal of the Acoustical Society of America*. **109(5)**: 2254-2259.

Klimley, A. P. and Brown, S. T. (1983) Stereophotography for the field biologist: Measurement of lengths and three-dimensional positions of free-swimming sharks. *Marine biology*. **74**: 175-85.

Lettevall, E. Richter, C. Jaquet, N. Slooten, E. Dawson, S. Whitehead, H. Christal, J. and Howard, P. (2002) Social structure and residency in aggregations of male sperm whales. *Canadian Journal of Zoology* **80**: 1189- 96.

Levenson, C. (1974) Source level and bistatic target strength of the sperm whale (*Physeter catodon*) measured from an oceanographic aircraft. *The Journal of the Acoustical Society of America*. **55**: 1100-1103.

Madsen, P. Wahlberg, M. and Mohl, B. (2002) Male sperm whale (*Physter macrocephalus*) acoustics in a high-latitude habitat: implications for echolocation and communication. *Behavioral Ecology and Sociobiology*. **53**: 31-41.

Madson, P. T. Carder, D. A. Au, W. W. L. Nachtigall, P. E. Mohl, B. and Ridgway, S. H. (2003) Sound production in neonate sperm whales (L). *The Journal of the Acoustical Society of America*. **113(6)**: 2988-2991.

Marcoux, M. Whitehead, H. and Rendell, L. (2006) Coda vocalizations recorded in breeding areas entirely produced by mature female sperm whales (*Physeter macrocephalus*). *Canadian Journal of Zoology*. **84**: 609-614.

Mathias, D. Thode, A. Straley, J and Folkert, K. (2009) Relationship between sperm whale (*Physeter macrocephalus*) click structure and size derived from videocamera images of a depredating whale (sperm whale prey acquisition). *The Journal of the Acoustical Society of America*. **125(5)**: 3444-3453.

Melnikov, V. (1997) The Arterial System of the Sperm Whale (*Physeter macrocephalus*). Journal of Morphology. **234**: 37-50.

Mikhail, E. M. Bethel, J. S. and McGlone, J. C. (2001) Introduction to Modern Photogrammetry. *John Wiley & Sons*. New York.

Miller, B. (under examination) Acoustic growth rates and three-dimensional localisation of sperm whales (*Physeter macrocephalus*) in Kaikoura, New Zealand. PhD thesis. University of Otago, New Zealand.

Mohl, B. Larsen, E. and Amundin, M. (1981) Sperm whale size determination: Outlines of an acoustic approach. *Fisheries Series*. **5**: 327–332.

Mohl, B. Wahlberg, M. Madsen, P. T. Miller, L. A. And Surlykke, A. (2000) Sperm whale clicks: Directionality and source level revisited. *The Journal of the Acoustical Society of America*. **107(1)**: 638-648.

Mohl , B. (2001) Sound transmission in the nose of the sperm whale *Physeter catodon*. A post mortem study. *Journal of Comparative Physiology A*. **187**: 335-340.

Møhl, B. Wahlberg, M. Madsen, P. T. Heerfordt, A. and Lund, A. (2003) The monopulsed nature of sperm whale clicks *The Journal of the Acoustical Society of America.* **114(2)**: 1143–1154.

Morris, R.J. (1973) The lipid structure of the spermaceti organ of the sperm whale (*Physeter catodon*). *Deep-Sea Research*. **20**: 911-916.

Morris, R. J. (1975) Further research into the Lipid structure spermaceti organ of the sperm whale (*Physeter catodon*). *Deep-Sea Research*. **22**: 483-89.

Nishiwaki, M. Ohsumi, S. and Maeda, Y. (1963) Change of form in the sperm whale accompanied with growth. *Whale research **Institute**, Tokyo*. **17**: 1-13.

Norris, K. S. and Harvey, G. W. (1972) A theory for the function of the spermaceti organ of the sperm whale (*Physeter macrocephalus* L) In: *Animal Orientation and Navigation*.(eds Galler, S.R.) NASA SP-262: 397-417.

Ohsumi, S. (1966) Sexual segregation of the sperm whale in the North Pacific. *Scientific Reports of the Whales Research Institute, Tokyo*. **23**: 1-25.

Pavan, G. Hayward, T. J. Borsani, J. F. Priano, M. Manghi, M. Fossati, C. and Gordon, J. (2000) Time patterns of sperm whale codas recorded in the Mediterranean Sea 1985-1996. *The Journal of the Acoustical Society of America*. **107(6)**: 3487-3495.

Perryman, W. L. and Lynn, M. S. (1993) Identification of geographic forms of common dolphins (*Delphinus delphis*). *Marine Mammal Science*. **9(2)**: 119-137.

Perryman, W. L. and Lynn, M. S. (2002) Evaluation of nutritive condition and reproductive status of migrating gray whales (*Eschrichtius robustus*) based on analysis of photogrammetric data. *Journal of Cetacean Research and Management*. **4(2)**: 155-164.

Perryman, W. L. and Westlake, R. (1998) A new geographic form of the spinner dolphin, *Stenella longirostris*, detected with aerial photogrammetry. *Marine Mammal Science.* **14(1)**: 38-50.

Ratnaswamy, M. J. and Winn, H. E. (1993) Photogrammetric Estimates of Allometry and Calf Production in Fin Whales, *Balaenoptera physalus*. *Journal of Mammalogy*. **74(2)**: 323-330.

Ray, C. G. Wartzok, D. and Taylor, G. (1984) Productivity and behaviour of bowheads, *Balaena mysticetus*, and white whales, *Delphinapterus leucas*, as determined from remote sensing. *Reports of the International Whaling Commission*. **6**: 199-209.

Rendell, L. E. and Whitehead, H. (2002) Vocal clans in sperm whales *(Physeter macrocephalus). Proceedings of the Royal Society **B***. **270**: 225-231.

Rendell, L. and Whitehead, H. (2004) Do sperm whales share coda vocalizations? insights into coda usage from acoustic size measurement. *Journal of Animal Behaviour*. **67(5)**: 865–874.

Rhinelander, M. Q. (2001). Acoustic measurement of sperm whale length. Master's thesis, University of Otago.

Rhinelander, M. Q. and Dawson, S. M. (2004) Measuring sperm whales from their clicks: stability of interpulse intervals and validation that they indicate whale length. *The Journal of the Acoustical Society of America*. **115**: 1826-31.

Rice, D. W. (1989) Sperm Whale *Physeter macrocephalus* Linnaeus, 1758. In: *Handbook of Marine Mammals* Vol. 4: *River Dolphins and the large Toothed Whales.* (eds Ridgway, S.H and Harrison, R.) London, Academic Press: 177-233.

Richard, K. R. Dillon, M. C. Whitehead, H. and Wright, J. M. (1996) Patterns of kinship in groups of free-living sperm whales *(Physeter macrocephalus)* revealed by multiple molecular genetic analyses. *Proceedings of the National Academy of Sciences*. **93**: 8792-8795.

Richter, C.F. Dawson, S.M. and Slooten, E. (2003) Sperm whale watching off Kaikoura, New Zealand: effects of current activities on surfacing and vocalisation patterns. Science for conservation 219, funded by Conservation Services Levy. *Department of Conservation, Wellington*: 78. *http://www.doc.govt.nz/upload/documents/science-and-technical/srs52.pdf*

Rowe, L. and Dawson, S. (2008) Laser photogrammetry to determine dorsal fin size in a population of bottlenose dolphins from Doubtful Sound, New Zealand. *Australian Journal of Zoology*. **56**: 239-248.

Teloni, V. Zimmer, W. M. X. Wahlberg, M. and Madsen, P. T. (2007) Consistent acoustic size estimation of sperm whales using clicks recorded from unknown aspects. *Journal of Cetacean research and Management*. **9**: 127-36.

Thode, A. Mellinger, D. K. Stienessen, S. Martinez, A and Mullin, K. (2002) Depth-dependent acoustic features of diving sperm whales (*Physeter macrocephalus*) in the Gulf of Mexico. *The Journal of the Acoustical Society of America*. **112(1)**: 308- 321.

Von Bertalanffy, L. (1938) A quantitative theory of organic growth. *Human Biology*. **10(2)**: 181 – 213.

Watkins, W. A. (1980) Acoustics and the behaviour of sperm whales. In: *Animal Sonar Systems*. (eds. Busnel, R.G. and Fish, J.F) Plenum, New York: 283–90.

Webster, T. Dawson, S. and Slooten, E. (2009) A simple laser photogrammetry technique for measuring Hector's dolphins (*Cephalorhynchus hectori*) in the field. *Marine Mammal Science*. In Press.

Whitehead, H. (2003) Sperm whales: social evolution in the ocean. *The University of Chicago Press*, Chicago.

Whitney, W. (1968) Observations of sperm whale sounds from great depths. *Marine Physical Laboratory, Scripps Institute of Oceanography*: 1–9. MPL-U-11/68.

Zimmer, W. M. X. Madsen, P. T. Teloni, V. Johnson, M. P. and Tyack, P. (2005[a]) Off-axis effects on the multi-pulse structure of sperm whale usual clicks with implications for the sound production. *The Journal of the Acoustical Society of America*. **118**: 3337-45.

Zimmer, W. M. X., Tyack, P., Johnson, M. P. and Madsen, P. T. (2005[b]) Three-dimensional beam pattern of regular sperm whale clicks confirms bent-horn hypothesis. *The Journal of the Acoustical Society of America*. **117**: 1473-85.

Appendix

Element of exterior orientation used in the *Australis* photogrammetry software

The three elementary rotation matrixes used in the *Australis* photogrammetry software are:

1. a positive rotation of angle φ around the z axis yielding the first rotation matrix

$$\mathbf{R}_{\varphi} = \begin{bmatrix} \cos\varphi & \sin\varphi & 0 \\ -\sin\varphi & \cos\varphi & 0 \\ 0 & 0 & 1 \end{bmatrix};$$

2. a positive rotation of angle θ around the x axis yielding the second rotation matrix

$$\mathbf{R}_{\theta} = \begin{bmatrix} 1 & 0 & 0 \\ 0 & \cos\theta & \sin\theta \\ 0 & -\sin\theta & \cos\theta \end{bmatrix};$$

3. a negative rotation of angle ω around the y axis yielding the third rotation matrix

$$\mathbf{R}_{\omega} = \begin{bmatrix} \cos\omega & 0 & \sin\omega \\ 0 & 1 & 0 \\ -\sin\omega & 0 & \cos\omega \end{bmatrix}.$$

Finally, the combination of the three elementary rotations yields

$$\begin{pmatrix} x_3 \\ y_3 \\ z_3 \end{pmatrix} = \underbrace{\mathbf{R}_{\omega}\mathbf{R}_{\theta}\mathbf{R}_{\varphi}}_{\mathbf{R}} \begin{pmatrix} x_0 \\ y_0 \\ z_0 \end{pmatrix},$$

where **R** is the the total rotation matrix. In the context of the *Australis* software, **R** is obtained from individual rotation angles as follow:

$$\mathbf{R} = \begin{bmatrix} \cos\varphi\cos\omega + \sin\varphi\sin\theta\sin\omega & \sin\varphi\cos\omega - \sin\theta\cos\varphi\sin\omega & \cos\theta\cos\omega \\ -\sin\varphi\cos\theta & \cos\varphi\cos\theta & \sin\theta \\ -\sin\omega\cos\varphi + \sin\varphi\sin\theta\cos\omega & -\sin\omega\sin\varphi - \sin\theta\cos\varphi\cos\omega & \cos\theta\cos\omega \end{bmatrix}.$$

Transformation of the exterior orientation parameters from camera 2 to camera 1.

The coordinates expressed with respect to the reference system attached to the calibration wall are represented by $\begin{pmatrix} x_0 \\ y_0 \\ z_0 \end{pmatrix}$. Those expressed with respect to the reference systems attached to camera 1 (Left camera) and camera 2 (Right camera) are represented by $\begin{pmatrix} x_1 \\ y_1 \\ z_1 \end{pmatrix}$ and $\begin{pmatrix} x_2 \\ y_2 \\ z_2 \end{pmatrix}$, respectively (Fig 6.1).

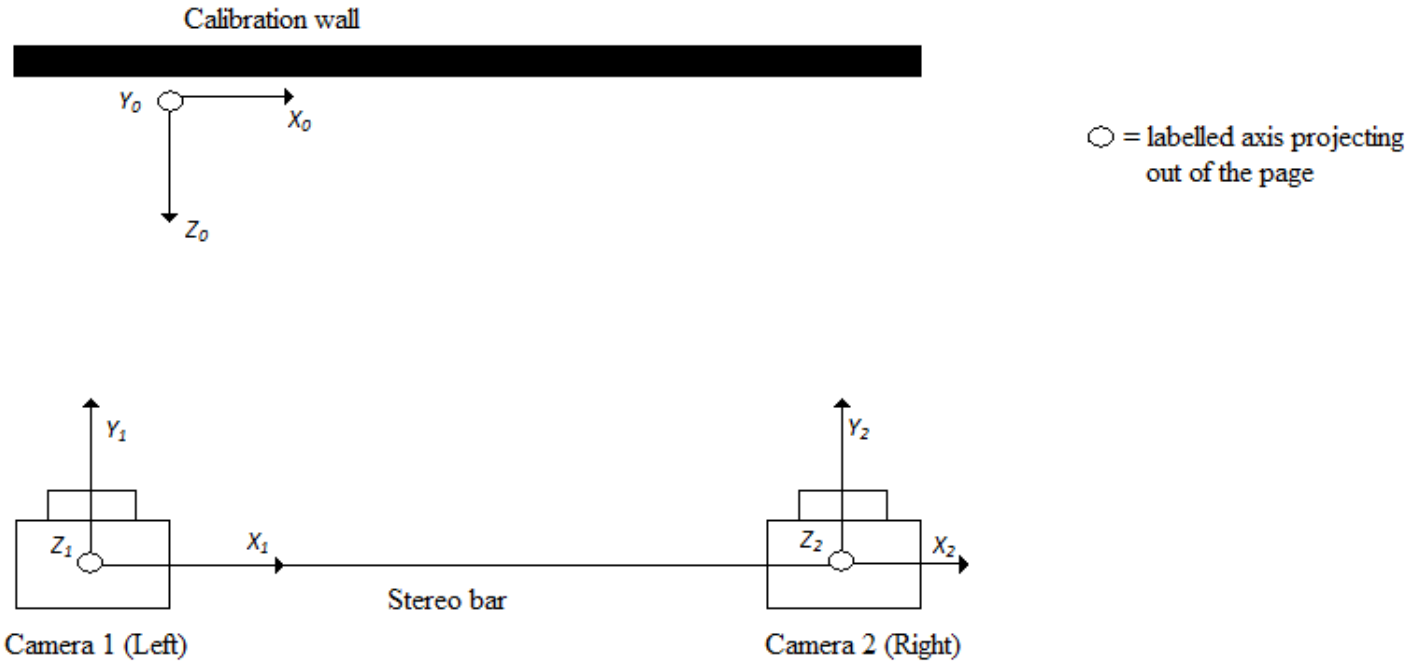

Figure. 6.1. Diagram showing the reference systems attached to each camera and the calibration wall.

The translation between the coordinate system attached to either camera and the wall is expressed as $\begin{pmatrix} a \\ b \\ c \end{pmatrix}$. The translation values as well as the elementary rotation angles for each camera with respect to the coordinate system of the wall are obtained from the bundle block adjustment performed in *Australis*. Thus, the transformation of coordinates from the system attached to the wall to that of camera 1 is given by

$$\begin{pmatrix} x_1 \\ y_1 \\ z_1 \end{pmatrix} = \mathbf{R}_1 \left[\begin{pmatrix} x_0 \\ y_0 \\ z_0 \end{pmatrix} - \begin{pmatrix} a_1 \\ b_1 \\ c_1 \end{pmatrix} \right].$$

The transformation of coordinates from the reference system attached to camera 2 to that of the calibration wall is given by

$$\begin{pmatrix} x_0 \\ y_0 \\ z_0 \end{pmatrix} = \mathbf{R}_2^{-1} \begin{pmatrix} x_2 \\ y_2 \\ z_2 \end{pmatrix} + \begin{pmatrix} a_2 \\ b_2 \\ c_2 \end{pmatrix}.$$

Combining both transformations, it is possible to express the transformation of coordinates from the reference system attached to camera 2 to that attached to camera 1 as follows:

$$\begin{pmatrix} x_1 \\ y_1 \\ z_1 \end{pmatrix} = \mathbf{R}_1 = \mathbf{R}_1\mathbf{R}_2^{-1}\begin{pmatrix} x_2 \\ y_2 \\ z_2 \end{pmatrix} + \mathbf{R}_1\begin{pmatrix} a_2 - a_1 \\ b_2 - b_1 \\ c_2 - c_1 \end{pmatrix}].$$

The previous equation is rearranged to identify a transformation of coordinates from the reference system attached to the camera 1 used as the new origin, to that attached to camera 2. It yields

$$\begin{pmatrix} x_2 \\ y_2 \\ z_2 \end{pmatrix} = \underbrace{(\mathbf{R}_1\mathbf{R}_2^{-1})^{-1}}_{\mathbf{R'}}\left[\begin{pmatrix} x_1 \\ y_1 \\ z_1 \end{pmatrix} - \underbrace{\mathbf{R}_1\begin{pmatrix} a_2 - a_1 \\ b_2 - b_1 \\ c_2 - c_1 \end{pmatrix}}_{\mathbf{t}}\right]),$$

where **R'** and **t** are the rotation matrix and the translation vector, respectively, from the reference system attached to camera 1 (used as the new origin) to that of camera 2. The exterior orientation of camera 2 is found relatively to camera 1 and independently to the calibration wall by deriving the three elementary rotation angle from **R'**. The new translation vector represents the main baseline along the x axis (i.e., the length of the aluminium bar), as well as residual offsets along the y and z axis.